The Instruments on the Chandra X-ray Observatory

Paul Plucinsky with the assistance of Dan Patnaude, Vinay Kashyap, Jeremy Drake and Mike Nowak (CXC)

Items I hope you remember:

1. Chandra's angular resolution distinguishes it from all other X-ray missions (75% encircled energy in a 1.0 arc second diameter region on-axis at 1.5 keV)
2. X-ray CCDs operate in the *photon counting* regime
3. The performance of ACIS and the HRC have evolved over the 21 year mission
4. Chandra should continue to operate for many years but we can not take it for granted

Outline of Topics:

High Resolution Mirror Assembly (HRMA)

- **Hughes Danbury Optical Systems/Kodak**
- **Telescope Scientist: Van Speybroeck (SAO)**

Two Focal Plane Instruments:

- **Advanced CCD Imaging Spectrometer (ACIS)**
  - **PSU/MIT/MIT LL/Martin Marietta PI: Garmire (PSU)**
  - **most of this talk will be about ACIS**
- **High Resolution Camera (HRC)**
  - **SAO PI: Murray (SAO)**

Two Grating Spectrometers:

- **High Energy Transmission Grating (HETG)**
  - **MIT PI: Canizares (MIT)**
- **Low Energy Transmission Grating (LETG)**
  - **SRON/MPE PI: Brinkman (SRON)**

Chandra Spacecraft

Prime Contractor (TRW, now NGAS), Lead subcontractor Ball Aerospace, NASA MSFC Program Office and Project Science

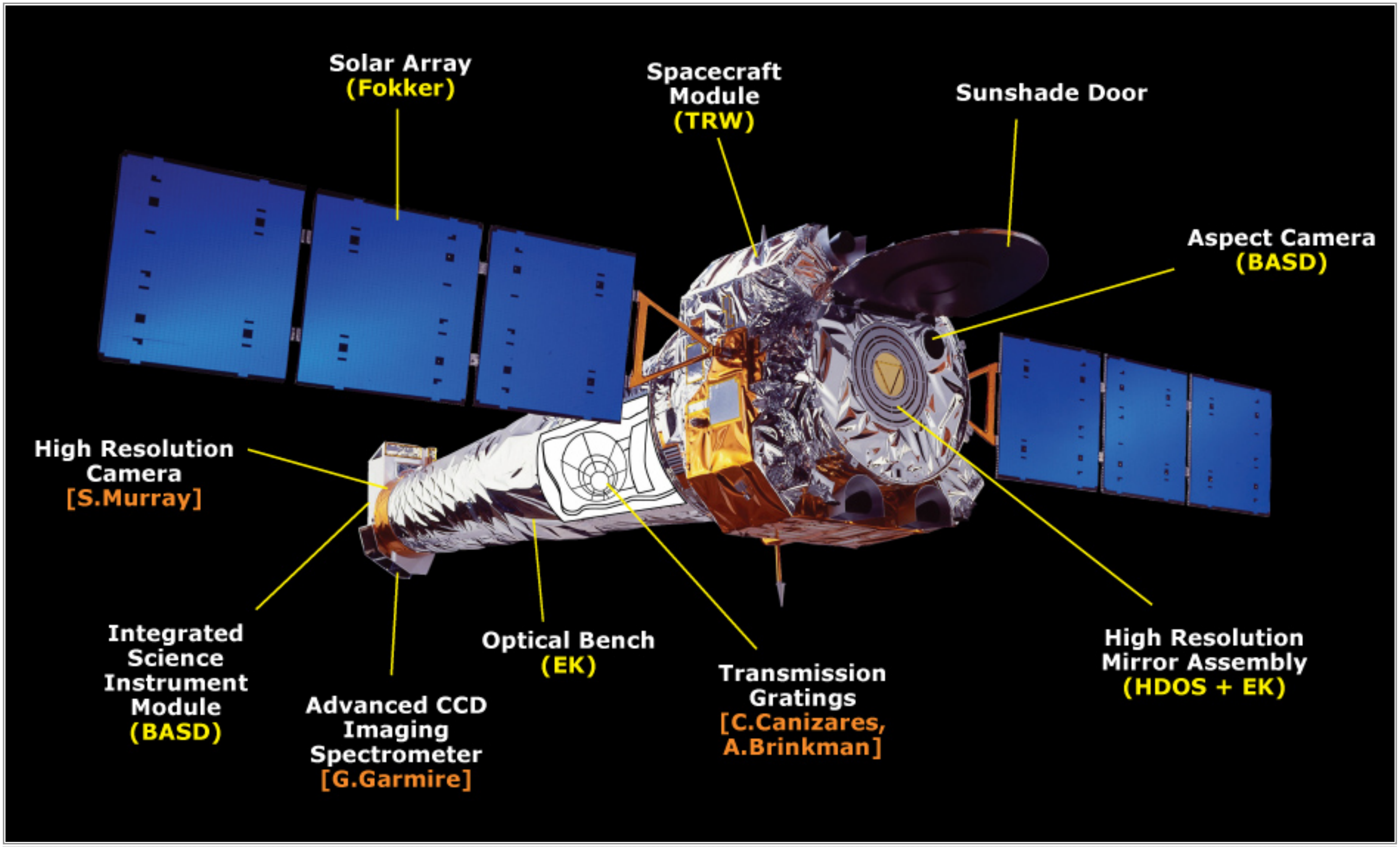

Chandra Operations

- Chandra is in a high Earth orbit, perigee altitude of 10,000 km, apogee altitude of 140,000 km (orbit evolves significantly with time, perigee altitude will reach a minimum of 1,100 km in 2023 before increasing again). This orbit allows long uninterrupted observations, although long observations are more difficult now given Chandra's thermal constraints.
- Chandra must use the Deep Space Network (DSN) for communications given this orbit. This limits us to 2-3 contacts per day, currently 2 per day. A typical contact is 1 hour.
- This COM schedule is a fundamental limiting factor in how quickly Chandra can respond to targets of opportunity. All commands must be built on the ground and uplinked to the satellite (other than the on-board safing sequences). Unlike the Swift satellite, Chandra can not maneuver autonomously.
- The Chandra operations control center (OCC) is in Burlington, MA ~15 miles from CfA. The OCC was located in Cambridge, MA for the first 19 years of the mission.

High Resolution Mirror Assembly

- mirror assembly consists of 4 paraboloid and hyperboloid pairs (Wolter Type I design)
- two reflections are needed to focus X-rays of different energies to the same point
- mirrors are polished Zerodur glass with an Ir coating to give the desired X-ray reflectivity. Mirror shells are thick. Mass is ~1,500 kg, entire satellite is ~5,000 kg.

the HRMA must be kept in a narrow range of temperatures on orbit (+22 +/- 2 C) to provide the best imaging performance

50% EE radius < 0.5 arc seconds

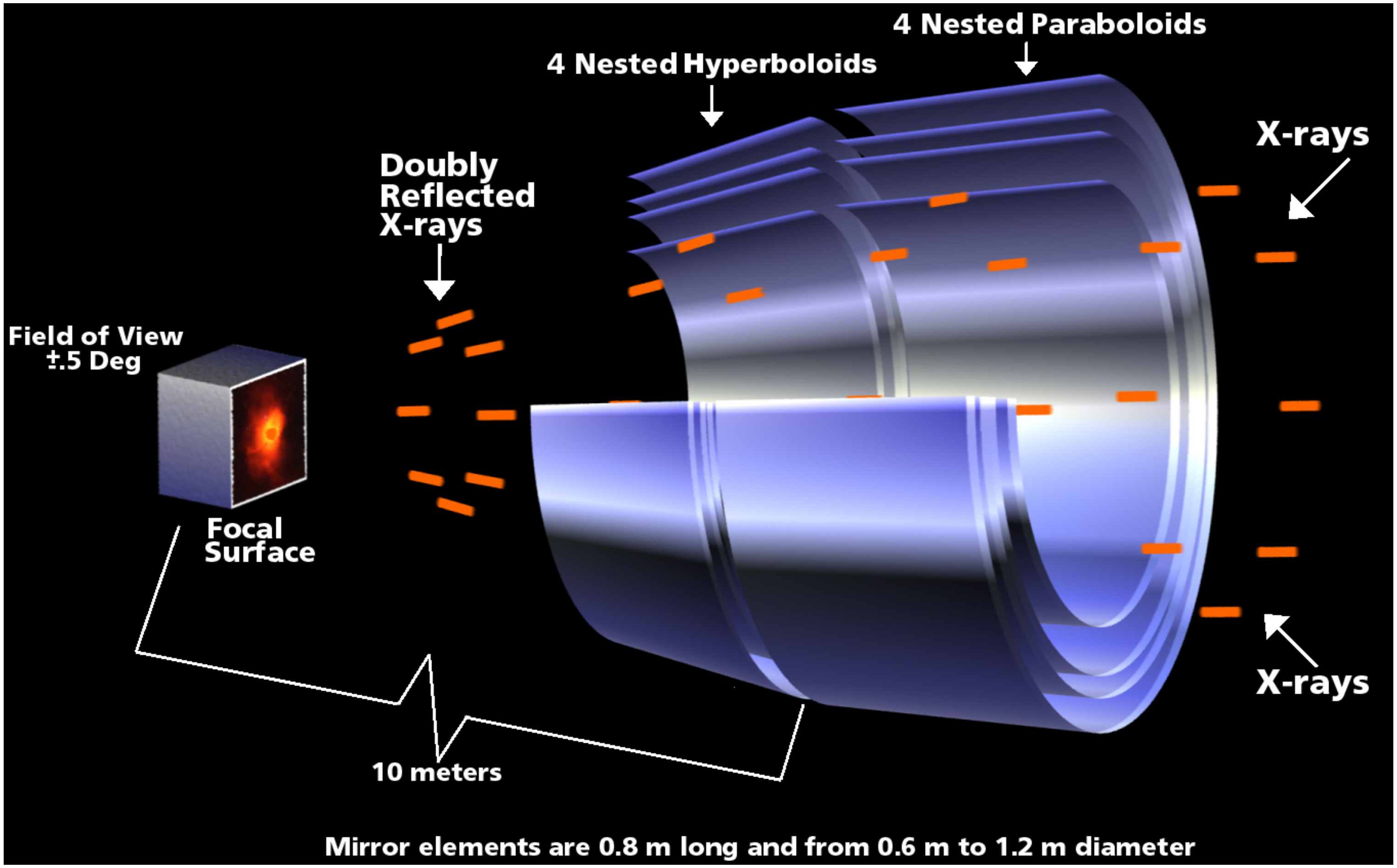

HRMA Effective Area and Resolution

- lower left plot show the effective area of the HRMA and various HRMA+instrument combinations. Note the units cm^{-2} !!!

- lower right plot show simulated images of a point source at different positions in the focal plane. Note that the angular resolution degrades significantly off-axis.

Chapter 4, https://cxc.harvard.edu/proposer/POG/html/index.html

ACIS-I FOV

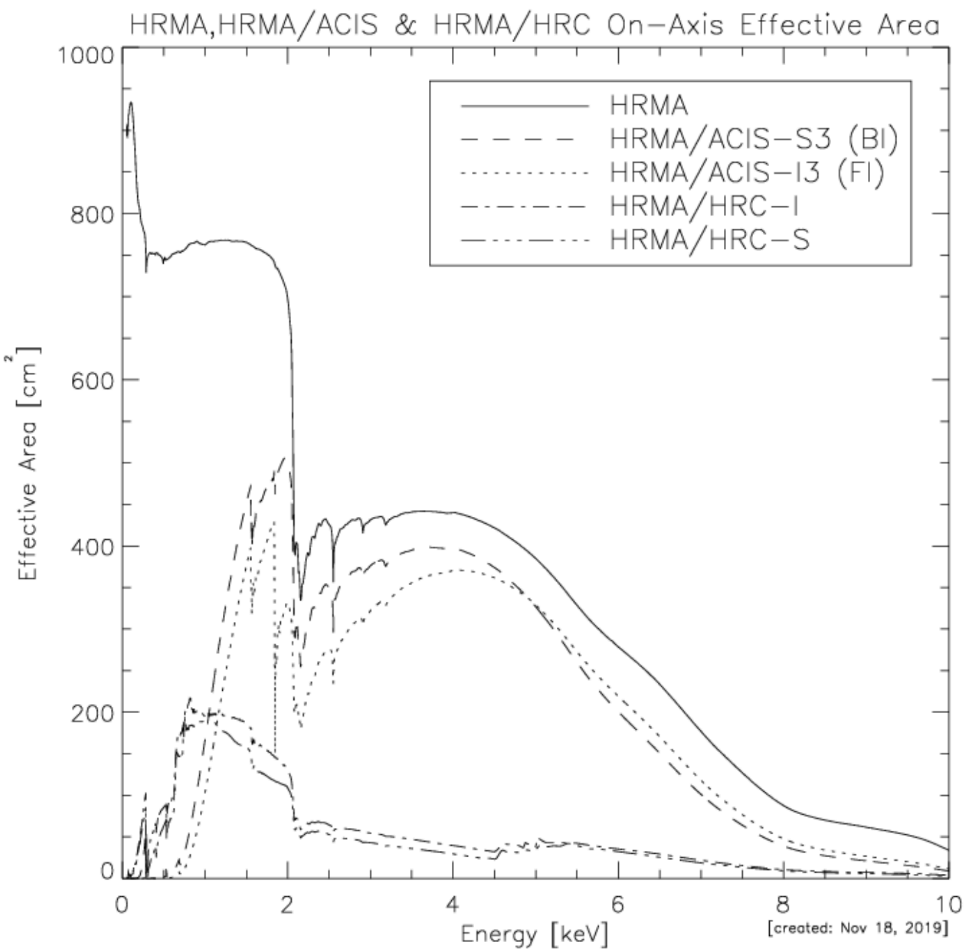

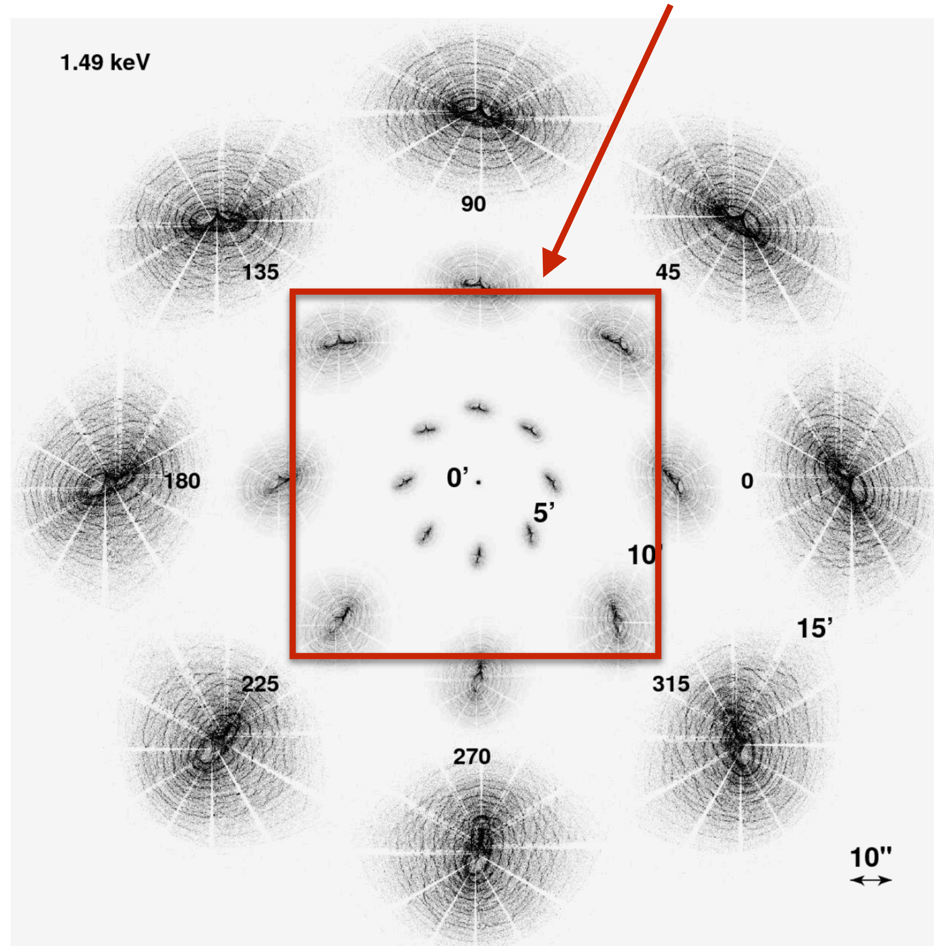

ACIS Focal Plane

10 CCDs arranged in two arrays, an imaging array called ACIS-I and a spectroscopy array called ACIS-S

8 Frontside-illuminated (FI) CCDs
2 Backside-illuminated (BI) CCDs

ACIS electronics can only read out 6 CCDs at a time

Both the I and S arrays are tilted to match the optimal focal surface

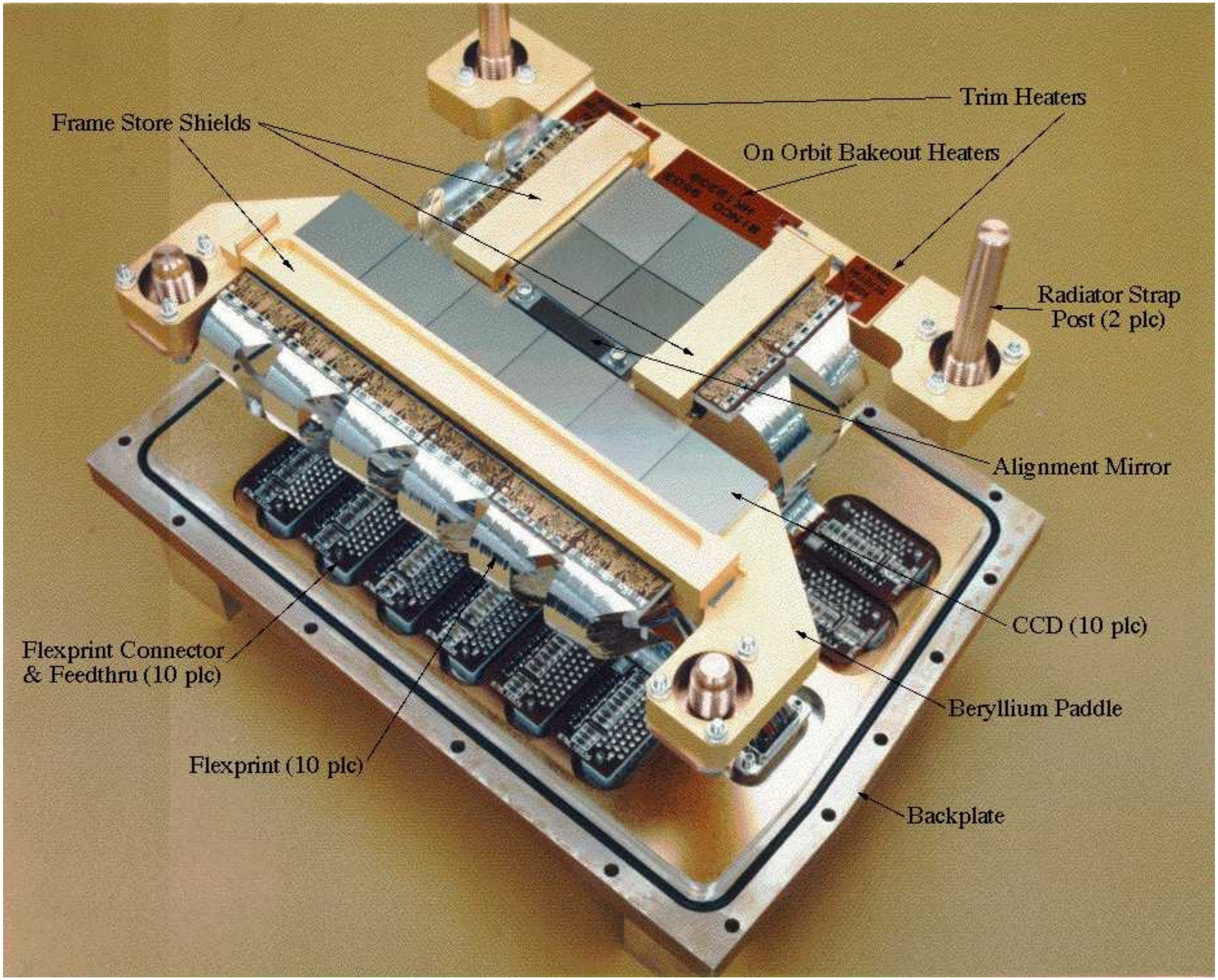

ACIS Focal Plane

Chapter 6, https://cxc.harvard.edu/proposer/POG/html/index.html

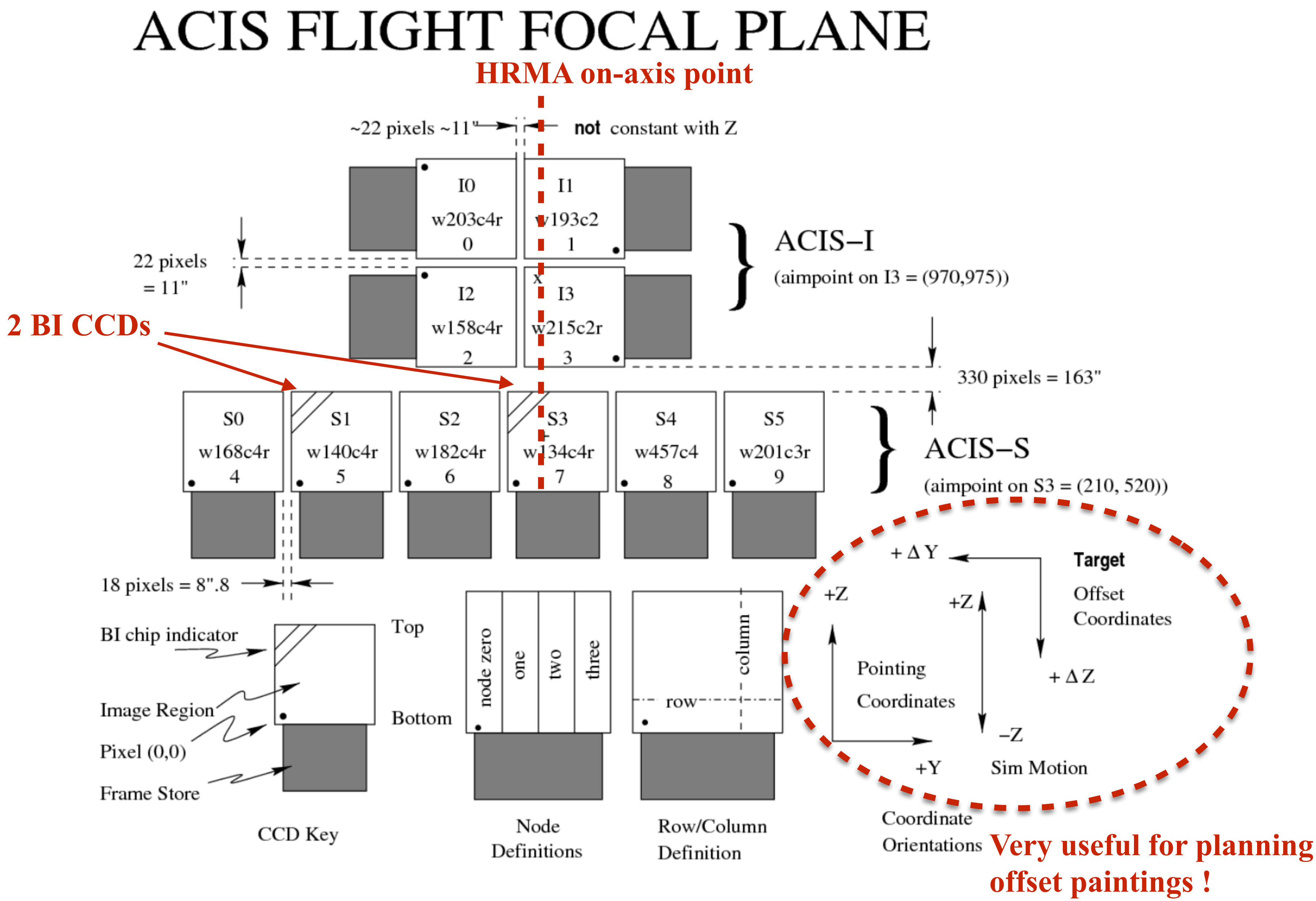

CCD Architecture

MIT Lincoln Laboratory CCDs
1024x1024 pixels, 24 µm pixels
Frame Store design CCDs, Image array is exposed to the incident radiation, the Frame Store array is shielded by an Au-plated Al cover
4 output nodes, 2-3e readout noise

CCDs can be clocked in:
Full Frame mode (largest area, longest frame time 3.2s)
Subarray Mode (smaller area, shorter frame time, as short as 0.4s)
Continuous Clocking Mode (2.85 ms row transfer time, sacrifices position information in one direction

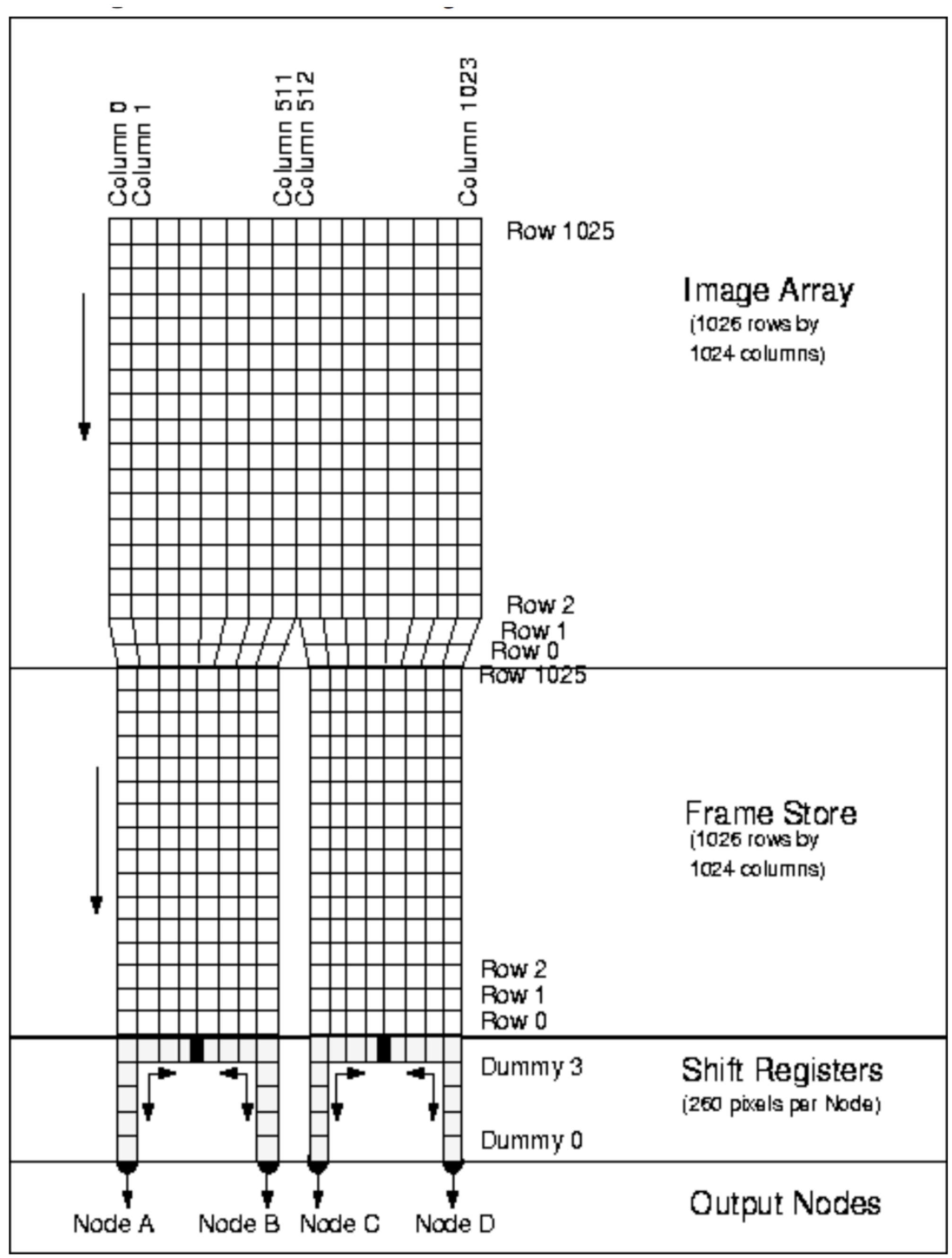

CCD Architecture

MIT Lincoln Laboratory CCDs
1024x1024 pixels, 24 µm pixels
Frame Store design CCDs, Image array is exposed to the incident radiation, the Frame Store array is shielded by an Au-plated Al cover
4 output nodes, 2-3e readout noise

CCDs can be clocked in:
Full Frame mode (largest area, longest frame time 3.2s)
Subarray Mode (smaller area, shorter frame time, as short as 0.4s)
Continuous Clocking Mode (2.85 ms row transfer time, sacrifices position information in one direction

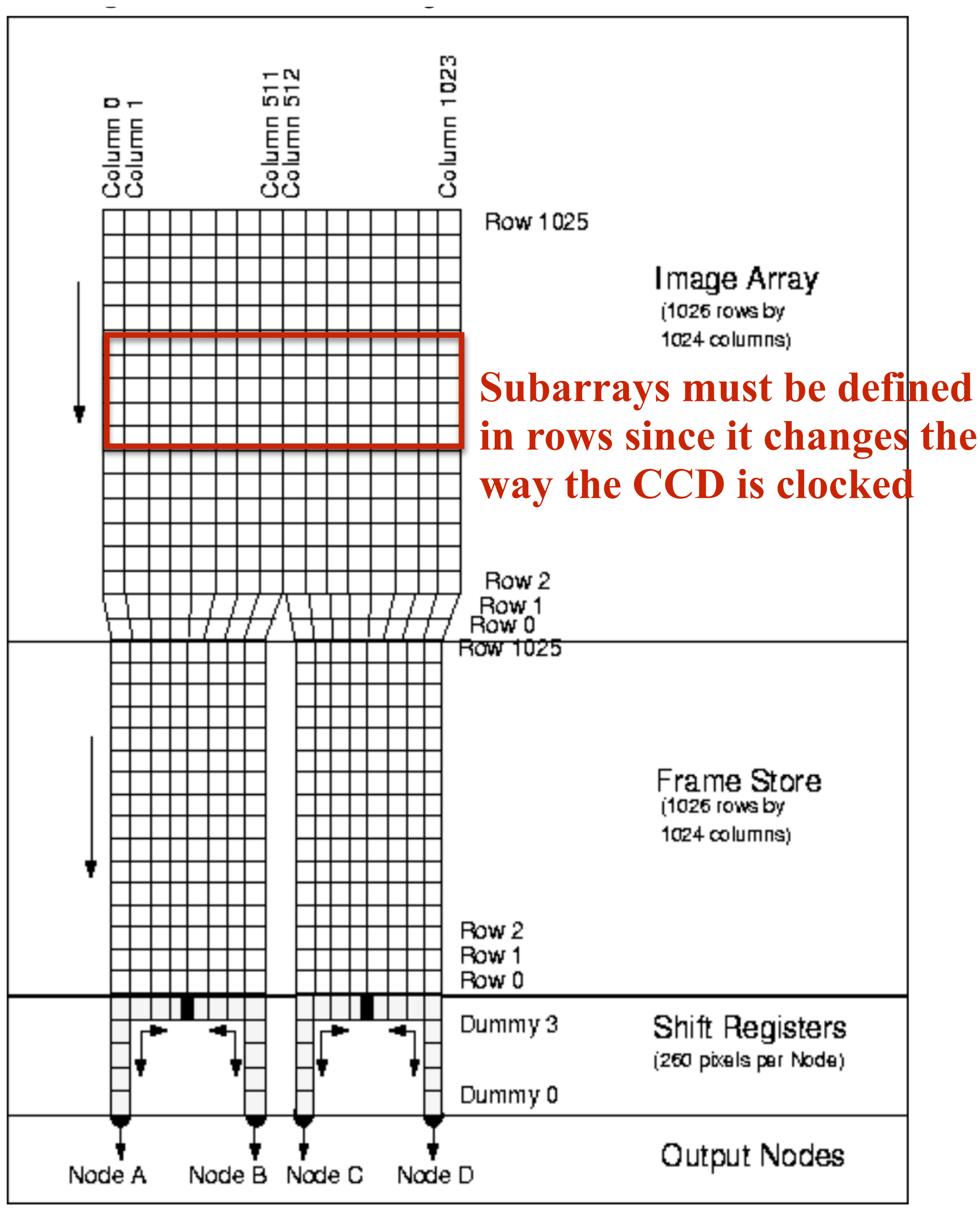

CCD Architecture

MIT Lincoln Laboratory CCDs
1024x1024 pixels, 24 µm pixels
Frame Store design CCDs, Image array is exposed to the incident radiation, the Frame Store array is shielded by an Au-plated Al cover
4 output nodes, 2-3e readout noise

CCDs can be clocked in:
Full Frame mode (largest area, longest frame time 3.2s)
Subarray Mode (smaller area, shorter frame time, as short as 0.4s)
Continuous Clocking Mode (2.85 ms row transfer time, sacrifices position information in one direction

Event filtering:
ACIS flight SW also allows spatial windows to select events based on position, pulse height and event grade
Subarrays and spatial windows can be used separately or together

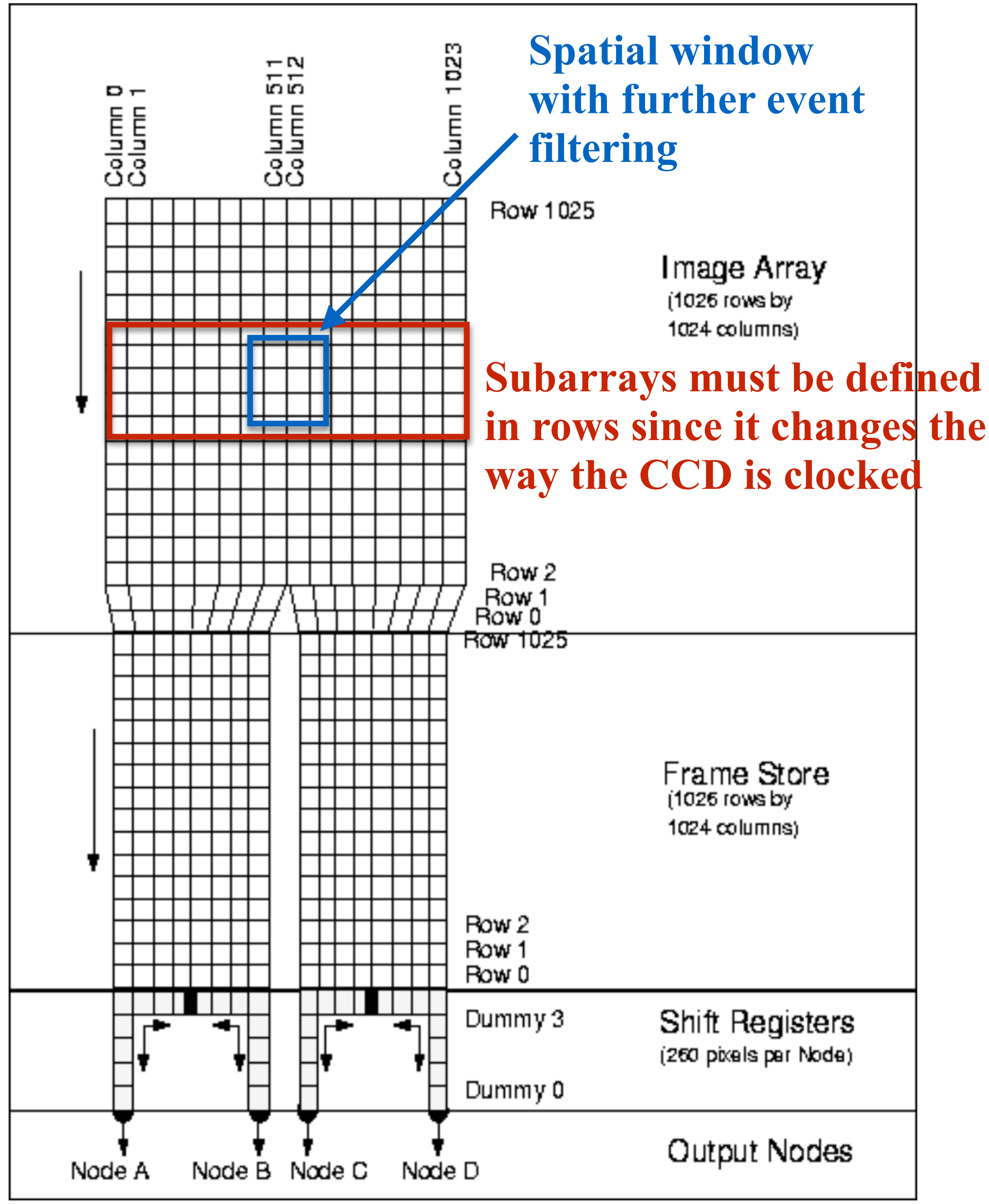

Timed Exposure Mode Readout

Integrate for 3.2s, this is the frame time

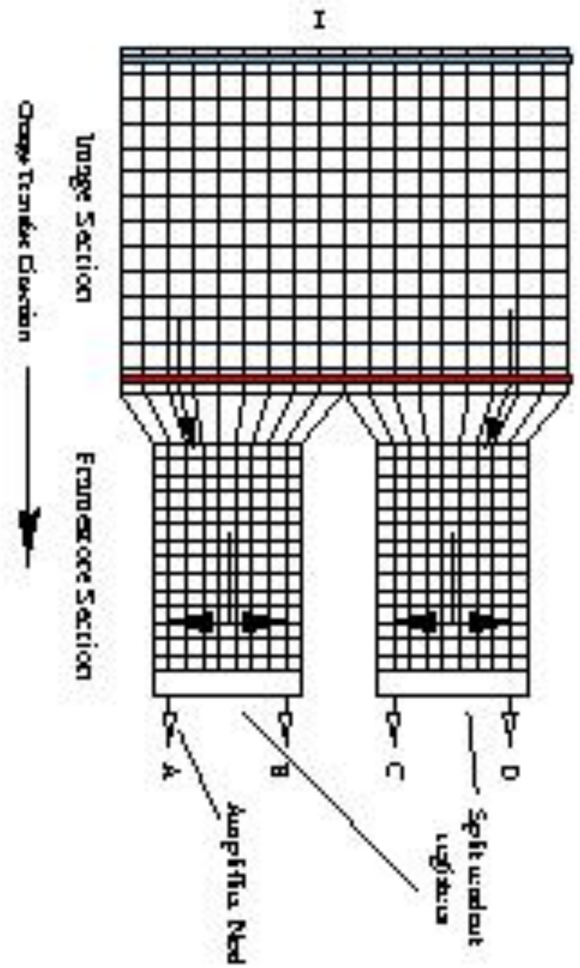

Image to Framestore Transfer 41ms

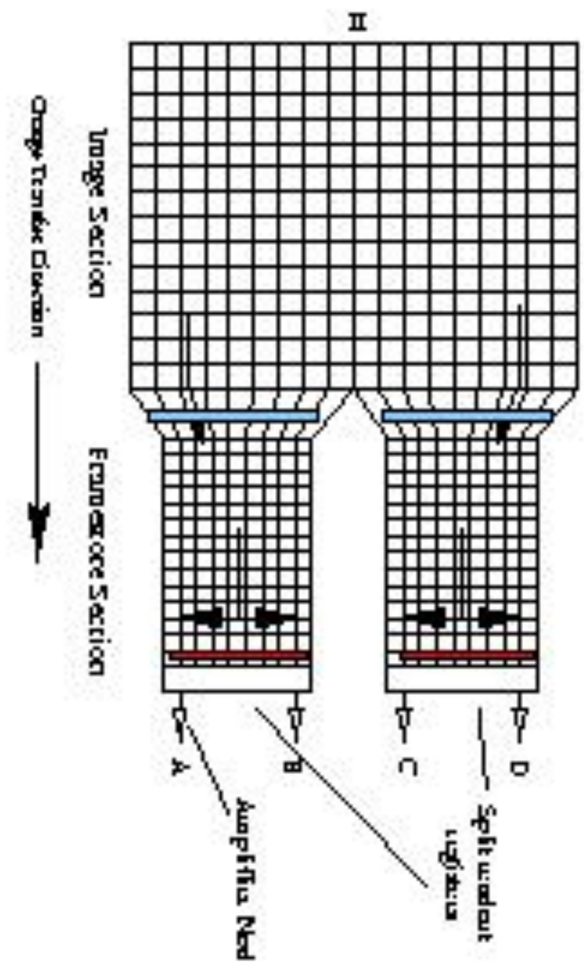

Framestore Readout 3.2s, Image array is accumulating the next exposure

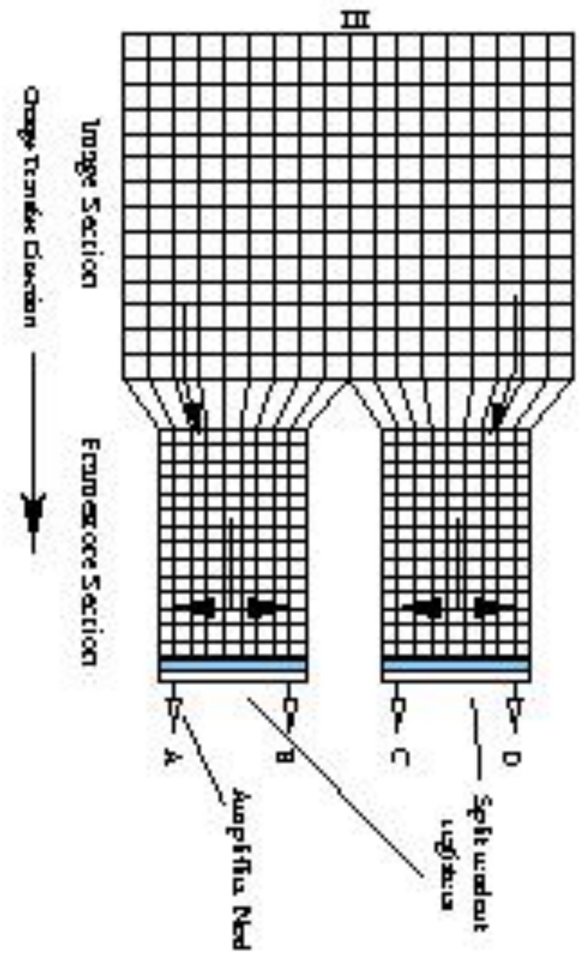

Events that interact with the CCD while the Image to Frame Store transfer is occurring result in an incorrect position assigned to the event and produce "transfer" streak events or "out-of-time" events.

Ground Calibration Data

I3 (FI CCD) subassembly data collected at MIT in 1997 !
Raw frame of data, every pixel is shown, most pixels have no charge.
This is the *photon-counting* regime.

O-Kα 0.525 keV

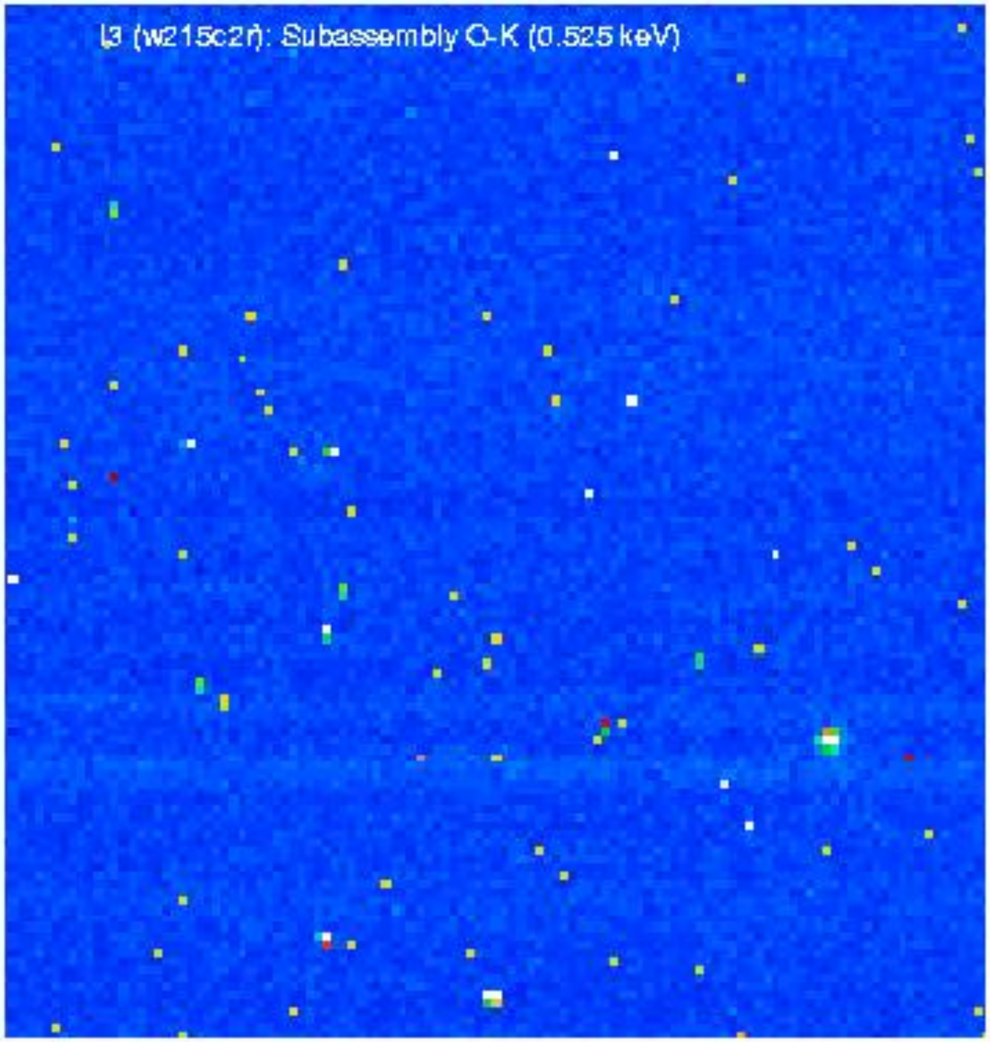

Cu-Kα 8.05 keV

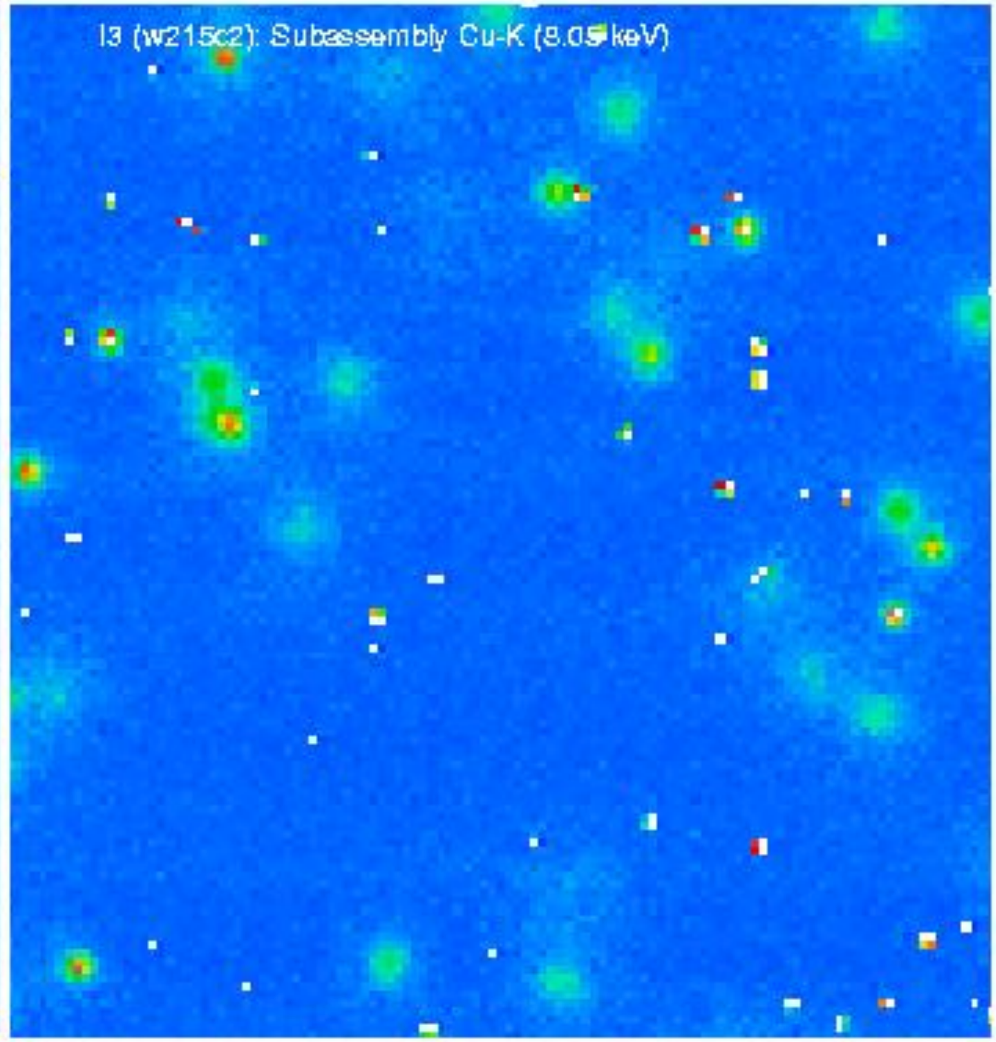

Ground Calibration Data

I3 (FI CCD) subassembly data collected at MIT in 1997 !

O-Kα 0.525 keV

Cu-Kα 8.05 keV

most O-Kα X-rays deposit charge in 1 or 2 pixels

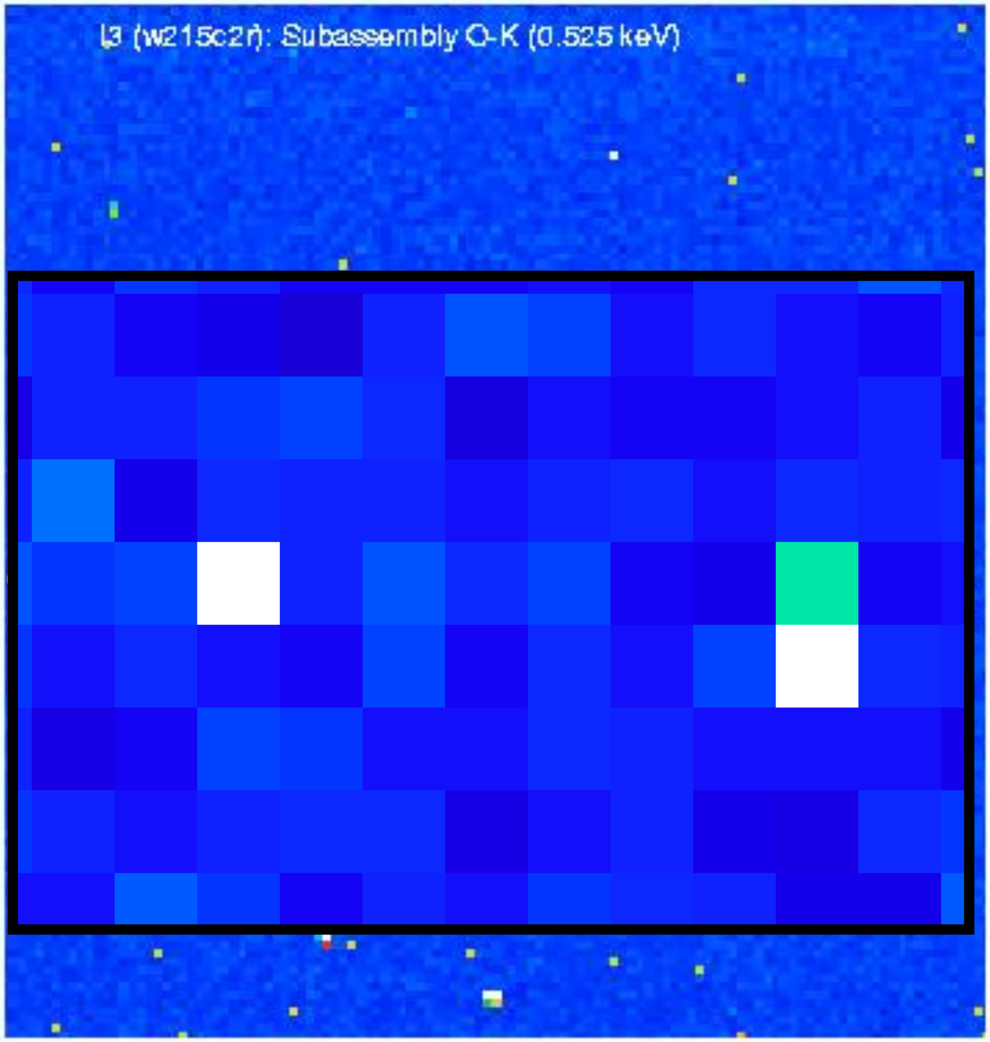

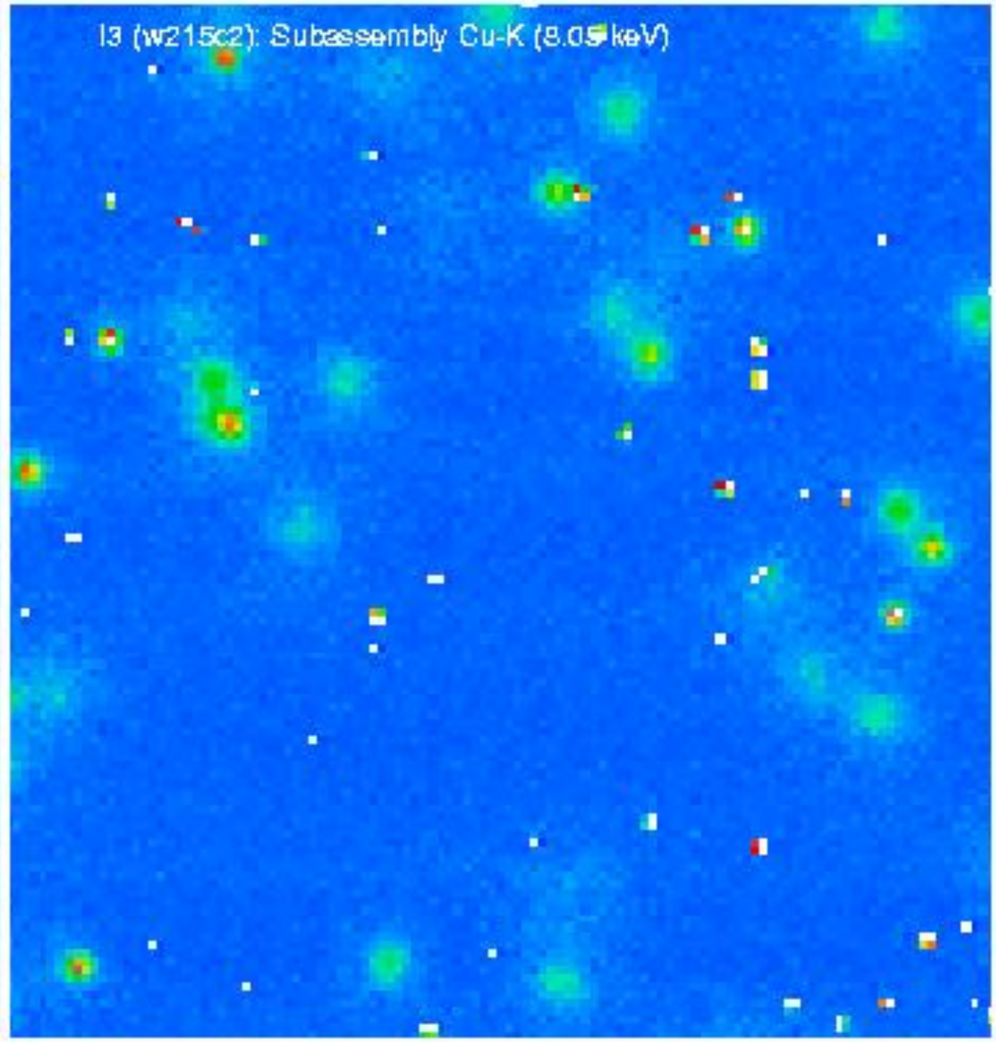

Ground Calibration Data

ACIS SW identifies an event in a 3x3 pixel island with the center of the event located at the pixel with the peak PH. If the charge in a neighboring pixel is above the “split threshold”, that charge is included in a summed PH for the event.

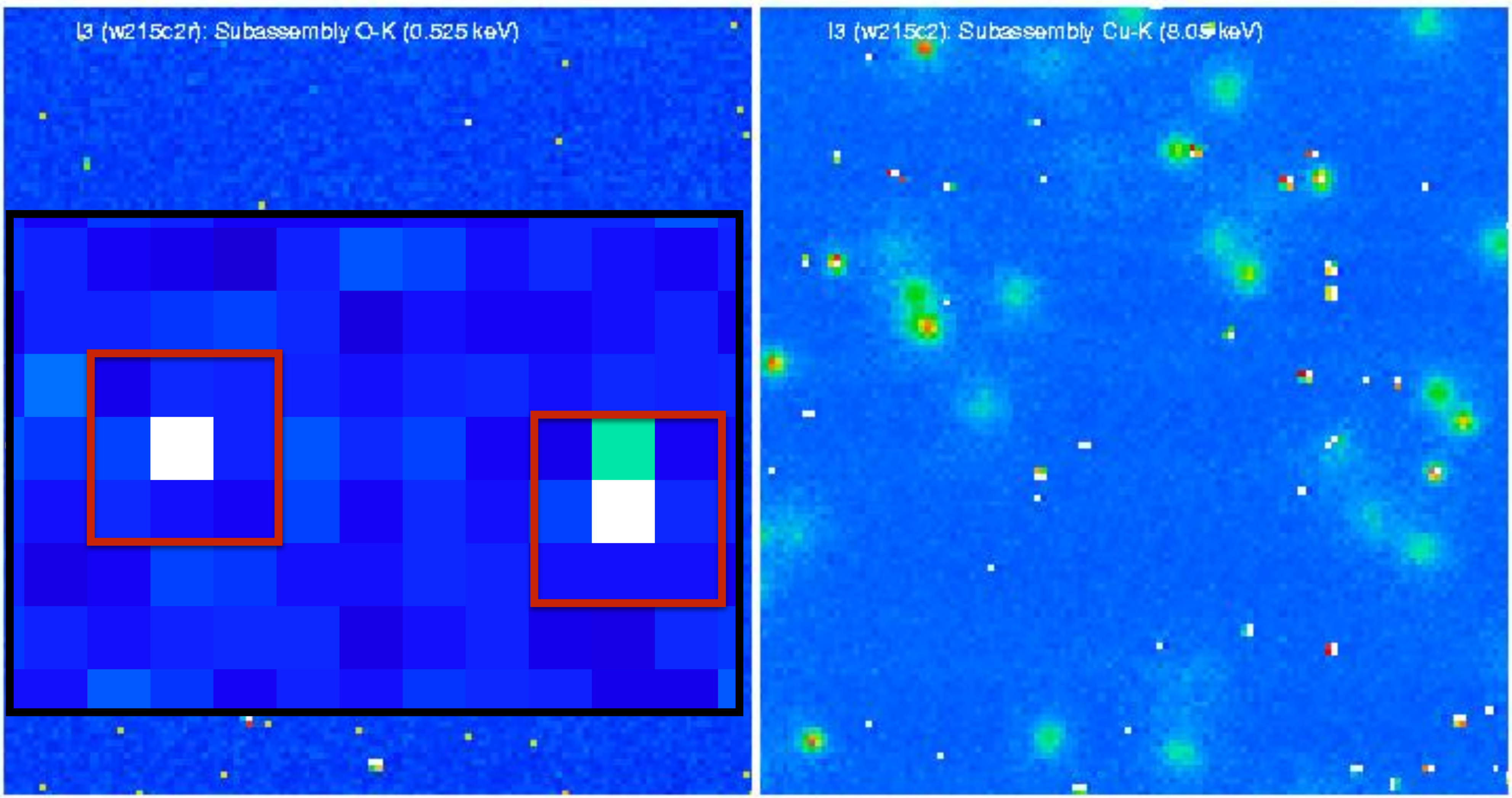

Ground Calibration Data

I3 (FI CCD) subassembly data collected at MIT in 1997 !

O-Kα 0.525 keV

Cu-Kα 8.05 keV

most Cu-Kα X-rays deposit charge in more than 1 pixel

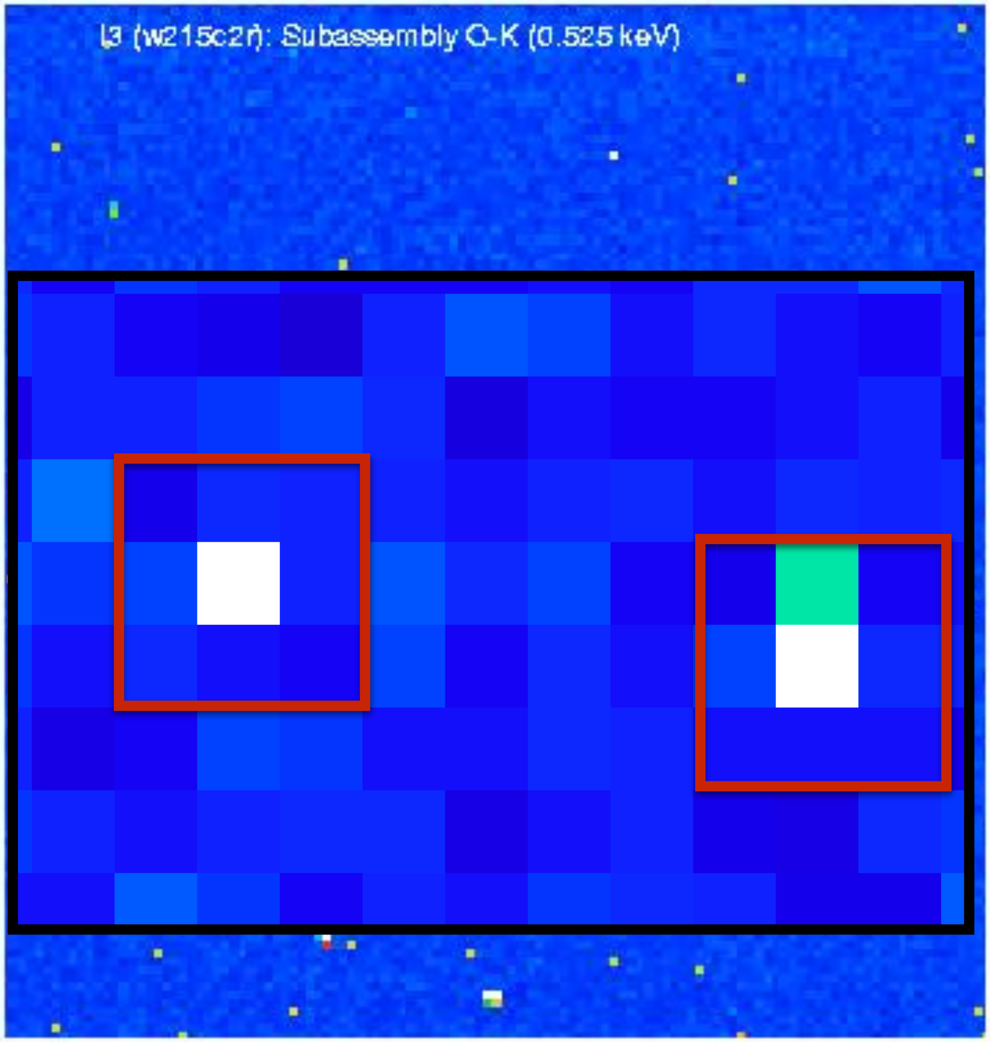

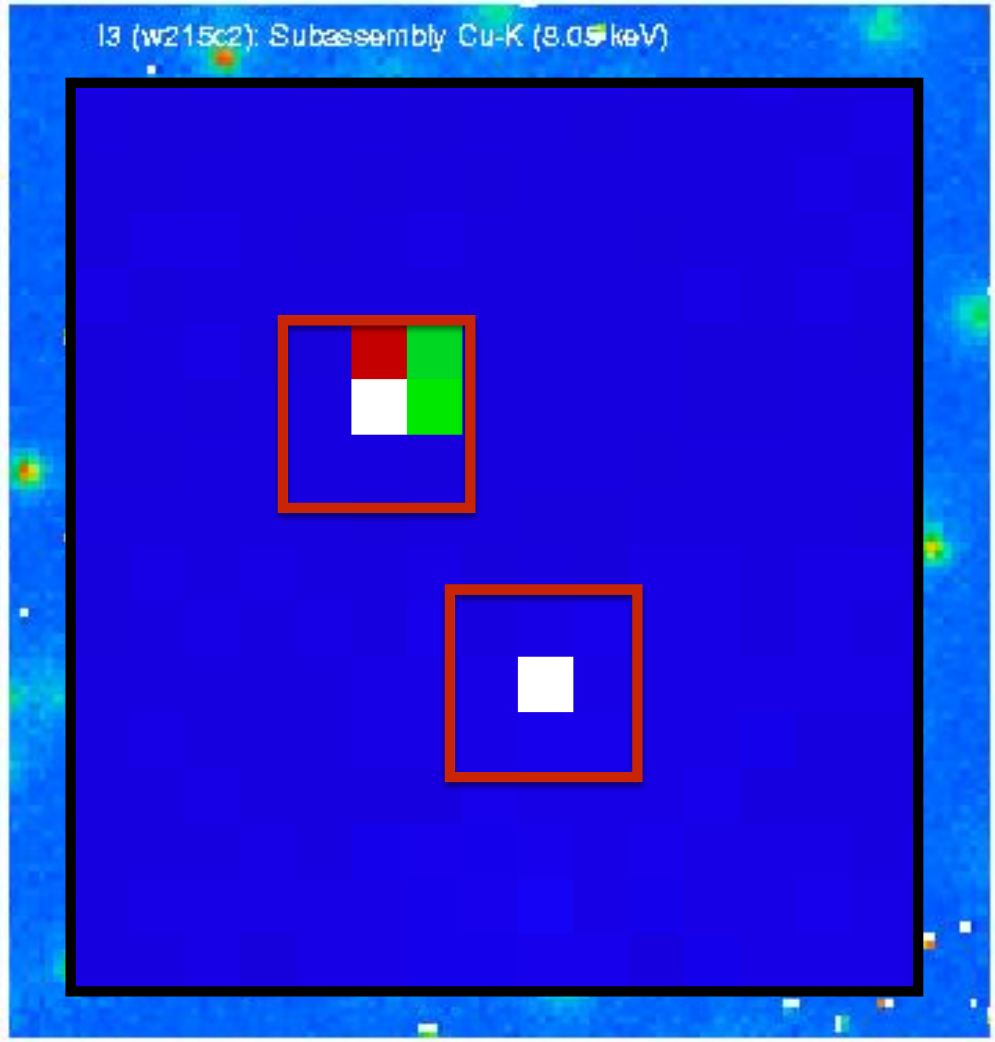

Raw Frames from Flight

I3 (FI CCD) and S3 (BI CCD) flight data collected June 2020.
Notice the large difference between the FI and BI CCDs for charged particles.

I3 FI CCD

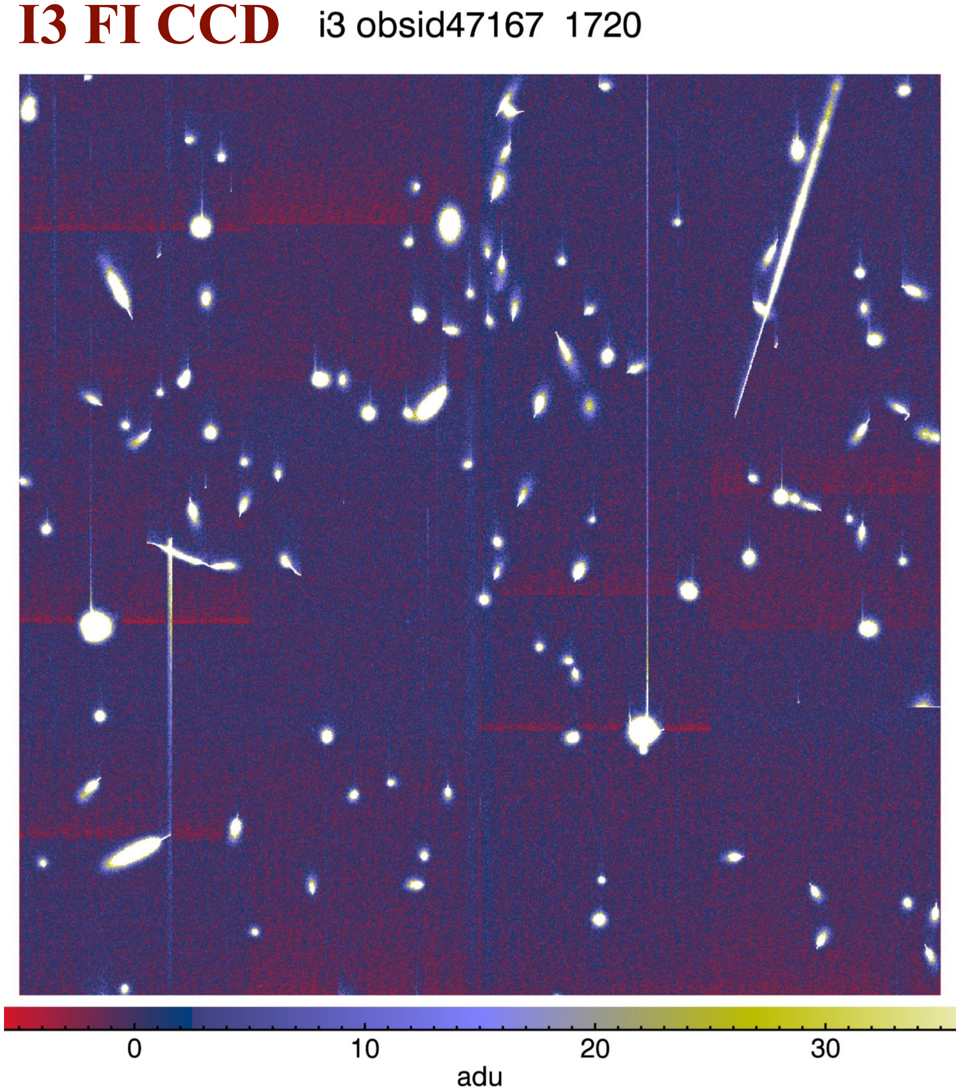

S3 BI CCD

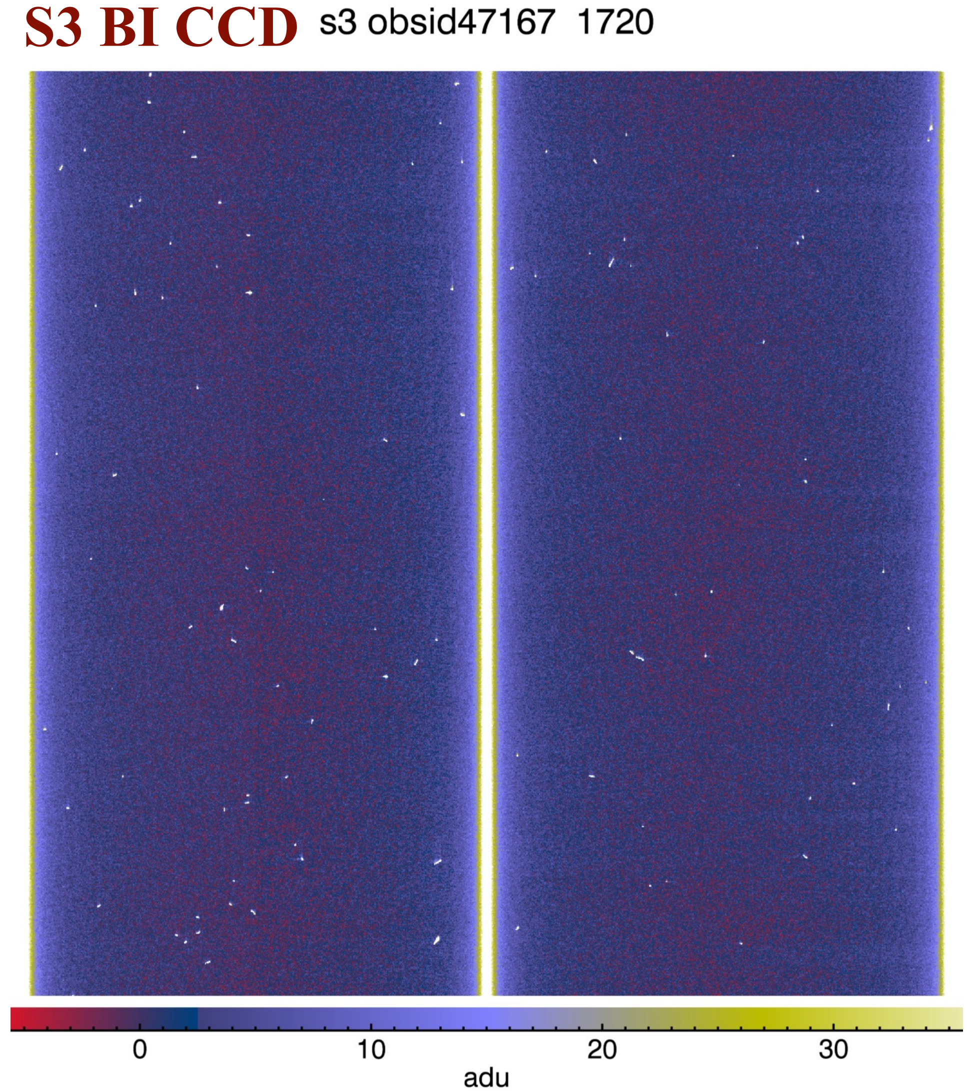

FI and BI CCD Architecture

ACIS flight SW identifies events and telemeters events to the ground. The fundamental ACIS data product is a *list of events*, from which images, spectra and light curves can be made. For each event, the following quantities are reported:
time (frame #), chipx, chipy, 9-25 PHs, Grade, summed PH

Grant, C. in Handbook of X-ray Astronomy, 2011

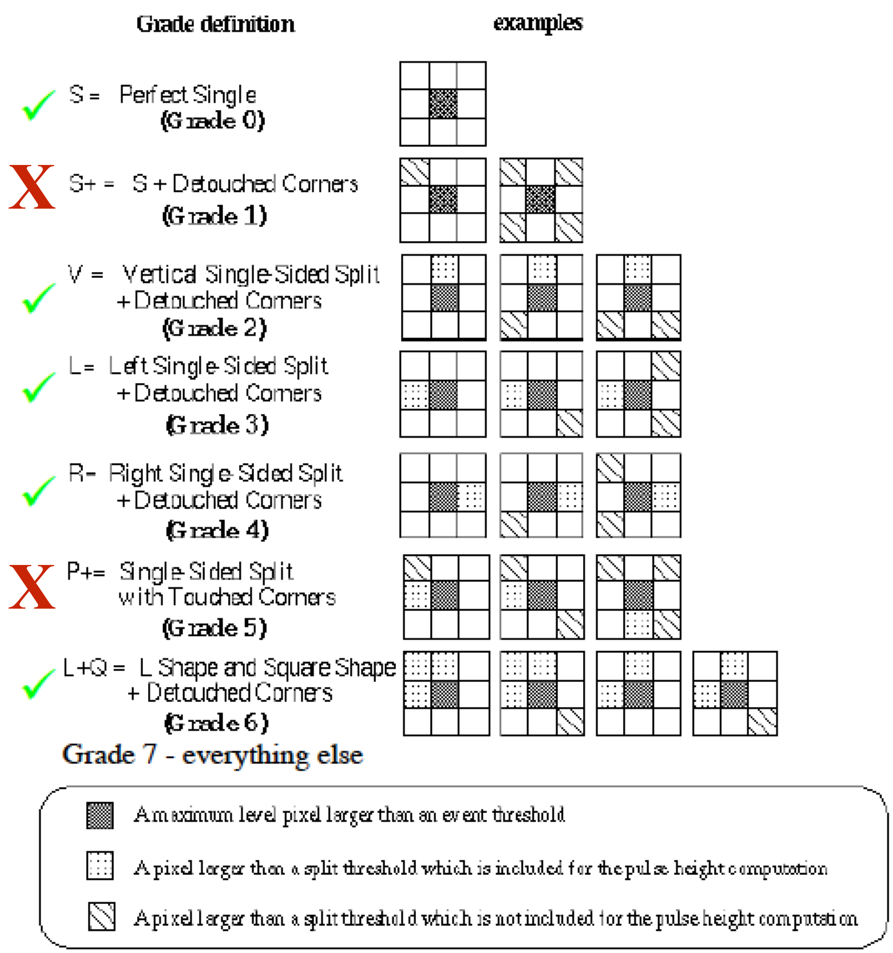

- Event grade can be used to discriminate between X-ray and cosmic ray events
- In general, X-ray events split into simpler/smaller shapes (single, singly-split) ✓
- Cosmic ray events are more complex
- ASCA code grades are one example
- Onboard grade filtering can further reduce telemetry
- Grade filtering can improve spectral resolution - split events are noisier than singles

FI and BI CCD Architecture

The ACIS FI CCDs have a large "field-free" region (substrate) in which charged particles can interact and create significant charge.

FI CCD

Townsley et al. 2002, NIM, 486, 716

BI CCD

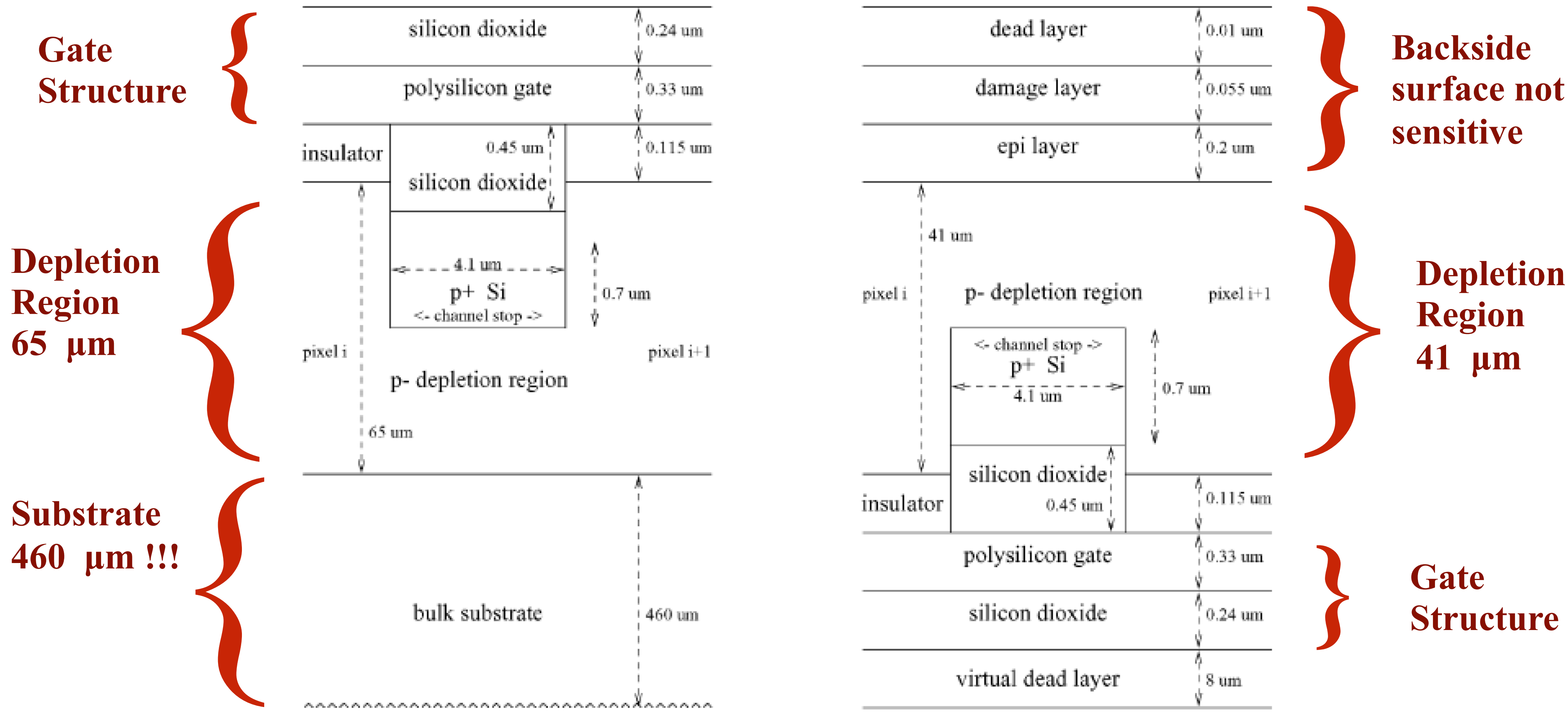

Fig. 4. Idealized geometry of an ACIS FI device (left) and an ACIS BI device (right) used in our model. Note that the layer thicknesses are not drawn to scale. "Insulator" is the silicon dioxide/nitride sandwich that makes up the gate insulator.

Bias Maps

The ACIS flight SW must calculate a "zero level" or a "bias" level, similar to a flat field for optical CCDs. The algorithm must exclude pixels with charge from X-ray events and charged particles. This is much more challenging for the FI CCDs.

FI CCD

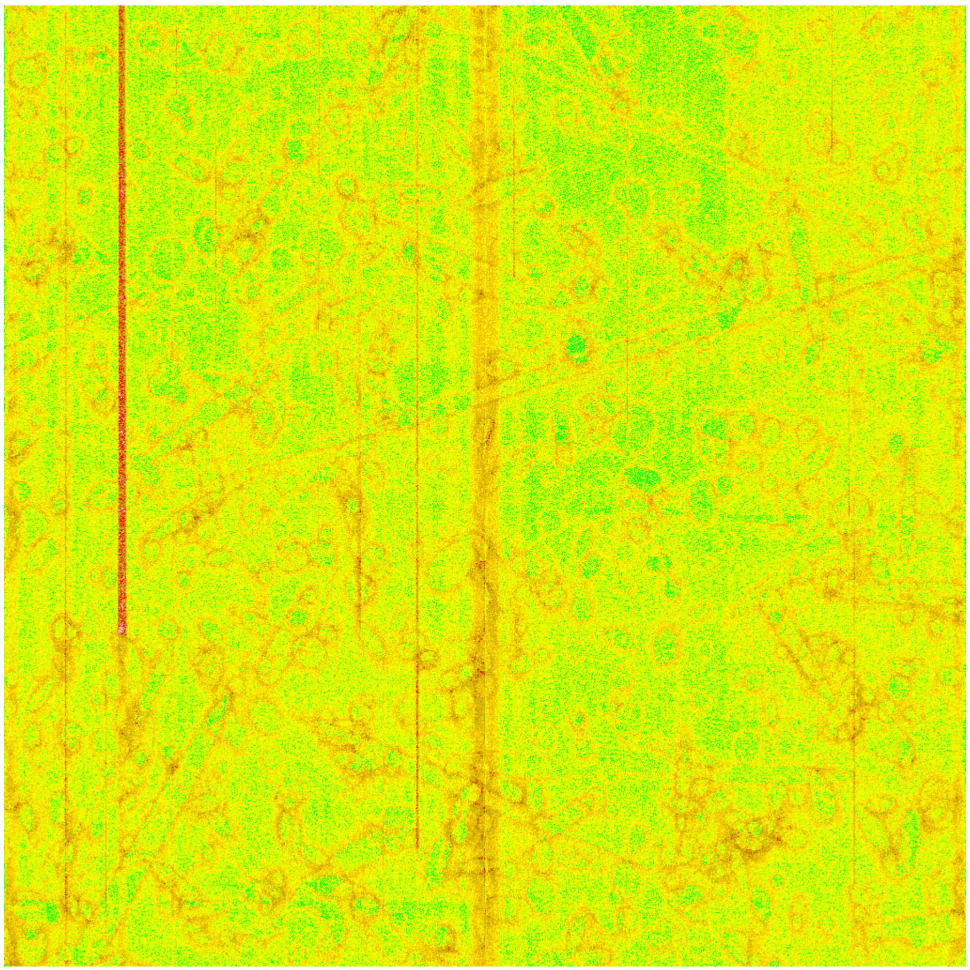

BI CCD

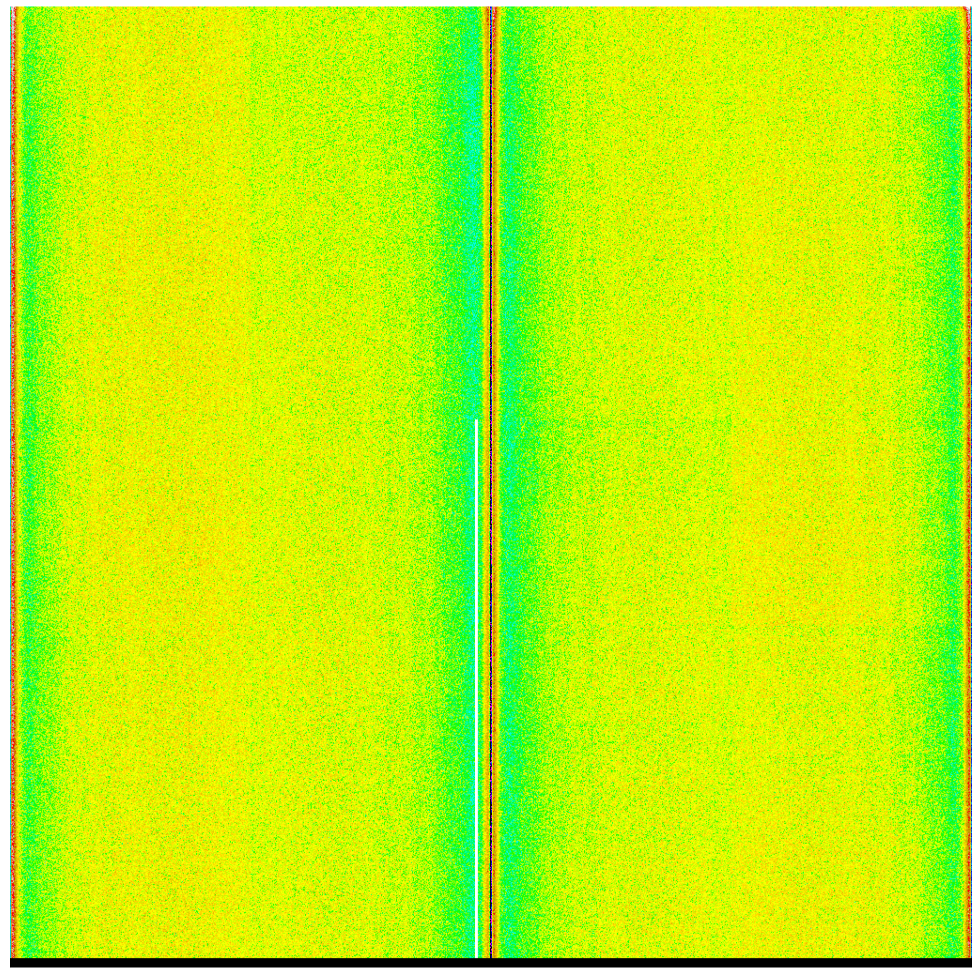

ACIS Spectral Response

Response of a CCD to monochromatic X-rays. Explanation for the features in the PH distribution.

Prigozhin et al. 2000, NIM, 439, 582

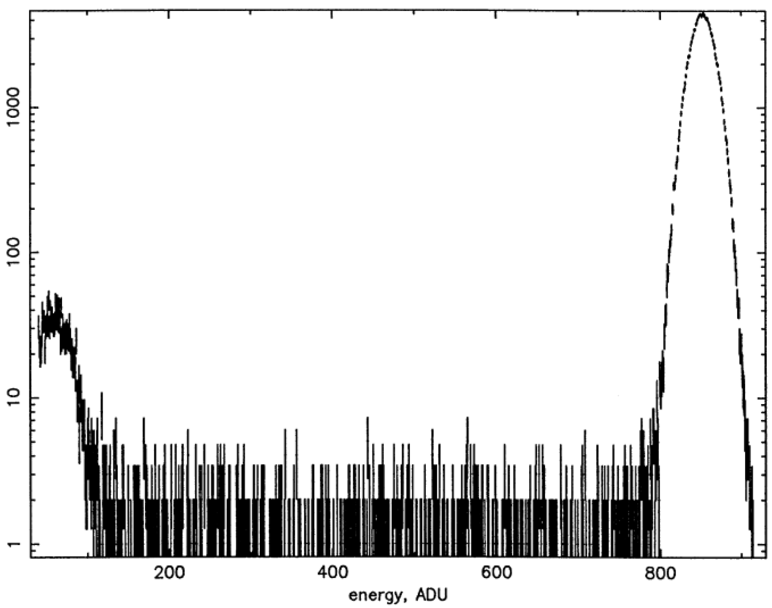

Fig. 1. Histogram of the CCD response to 1700 eV X-rays.

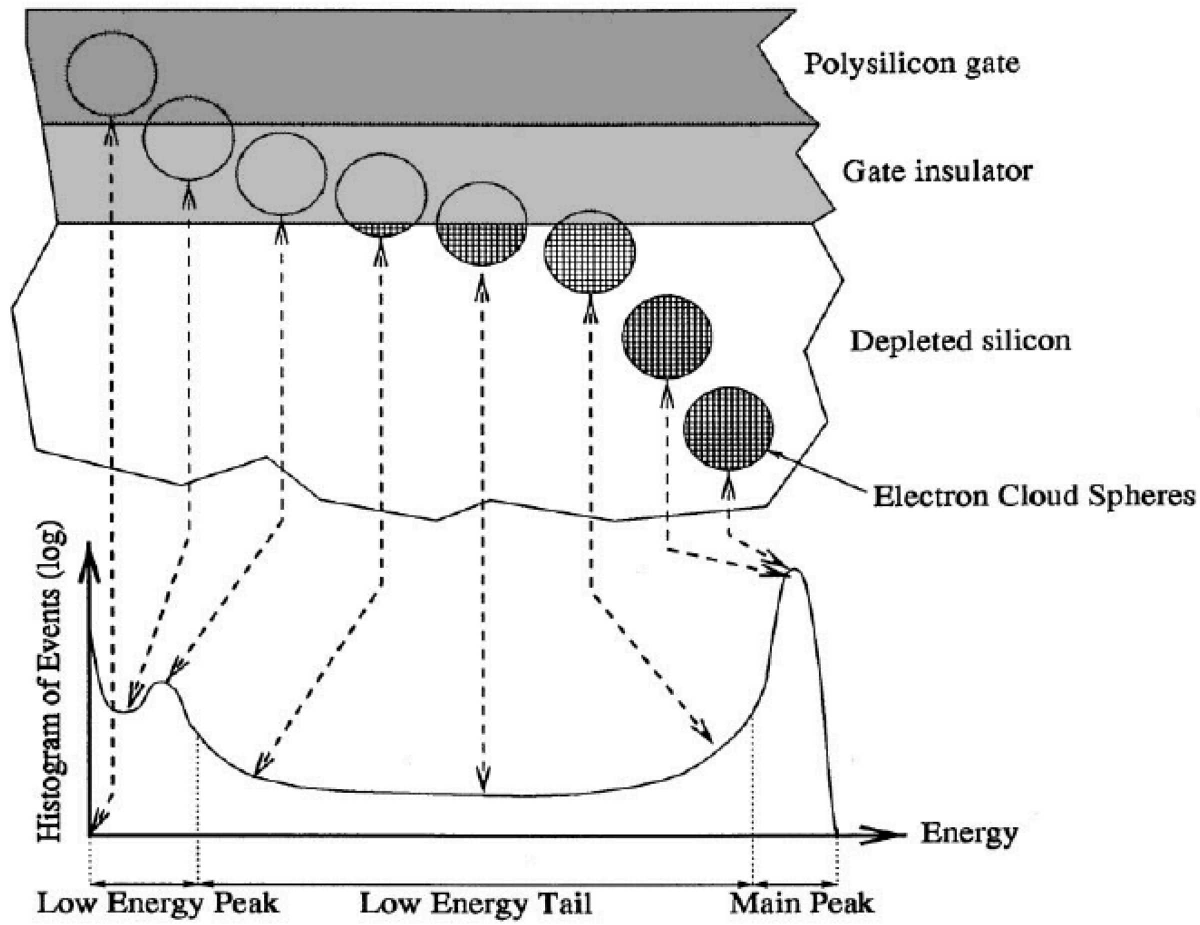

ACIS Spectral Response

Bautz et al. 1999, NIM, 436, 40

Response to an Fe55 source.

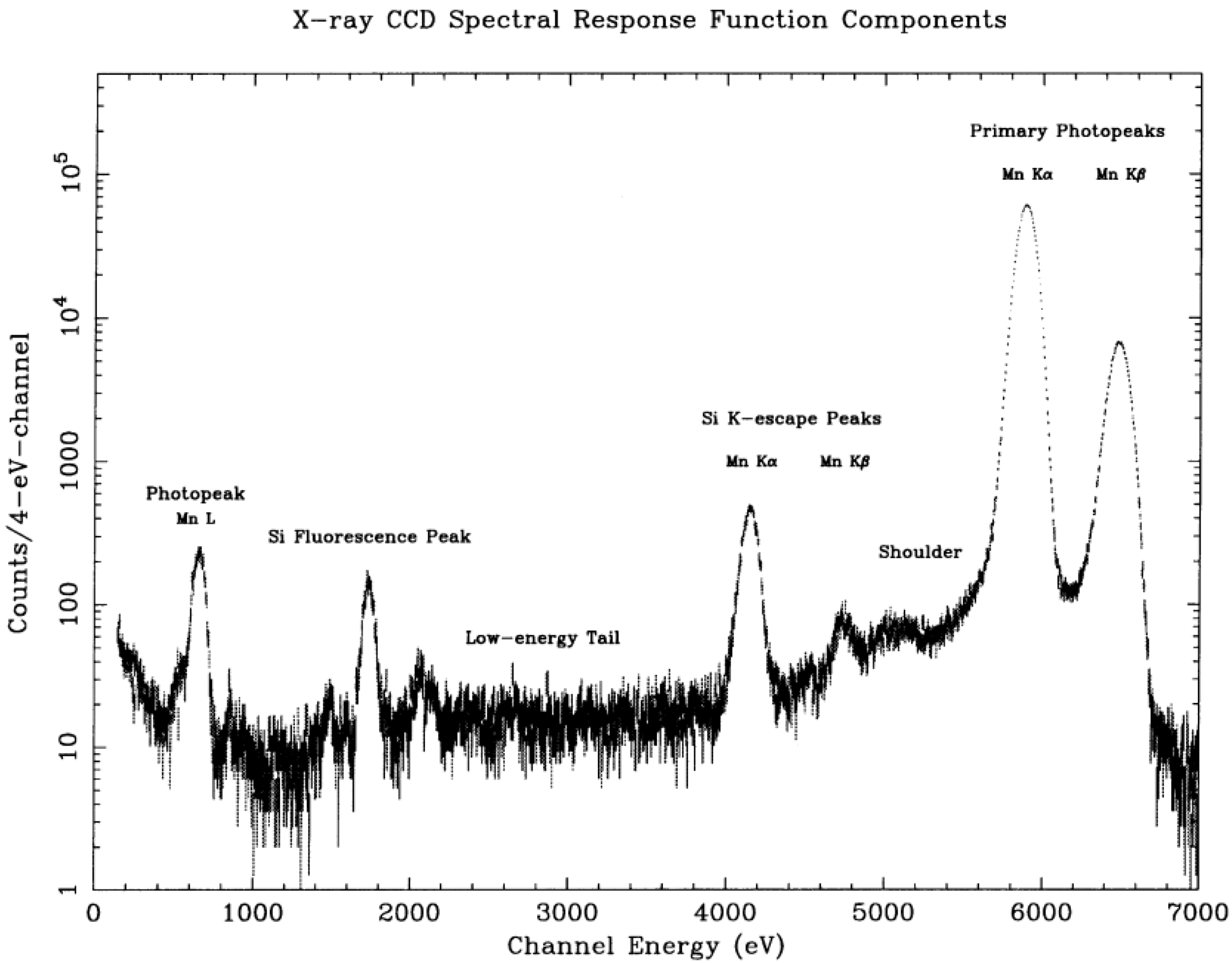

Fig. 1. X-ray CCD spectral redistribution function at 5.9 keV.

Charge Transfer Inefficiency

The ACIS FI CCDs unfortunately suffered a large amount of radiation damage in the first two months of the mission until we understood that ~100 keV proton scatter off of the HRMA with a significant efficiency. The BI CCDs were unaffected.

Townsley et al. 2002, NIM, 486, 751

CTI correction is applied to all data in the standard processing

no CTI correction

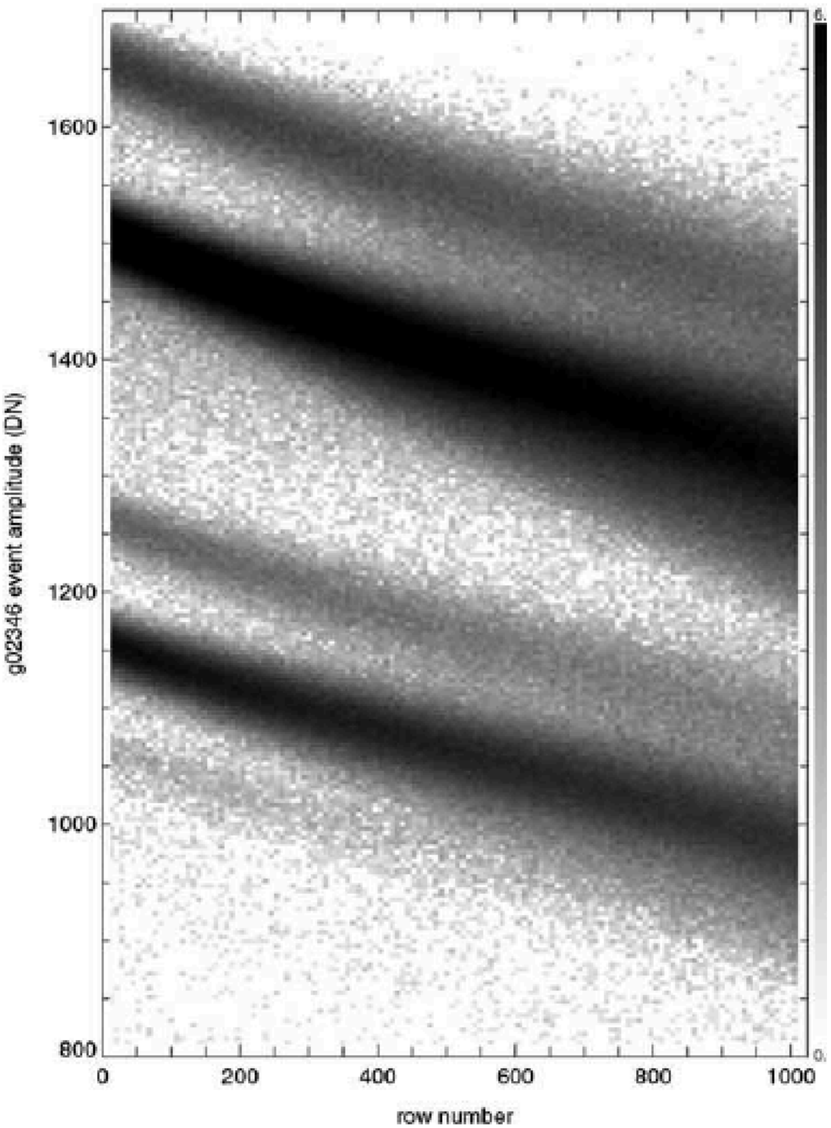

CTI correction

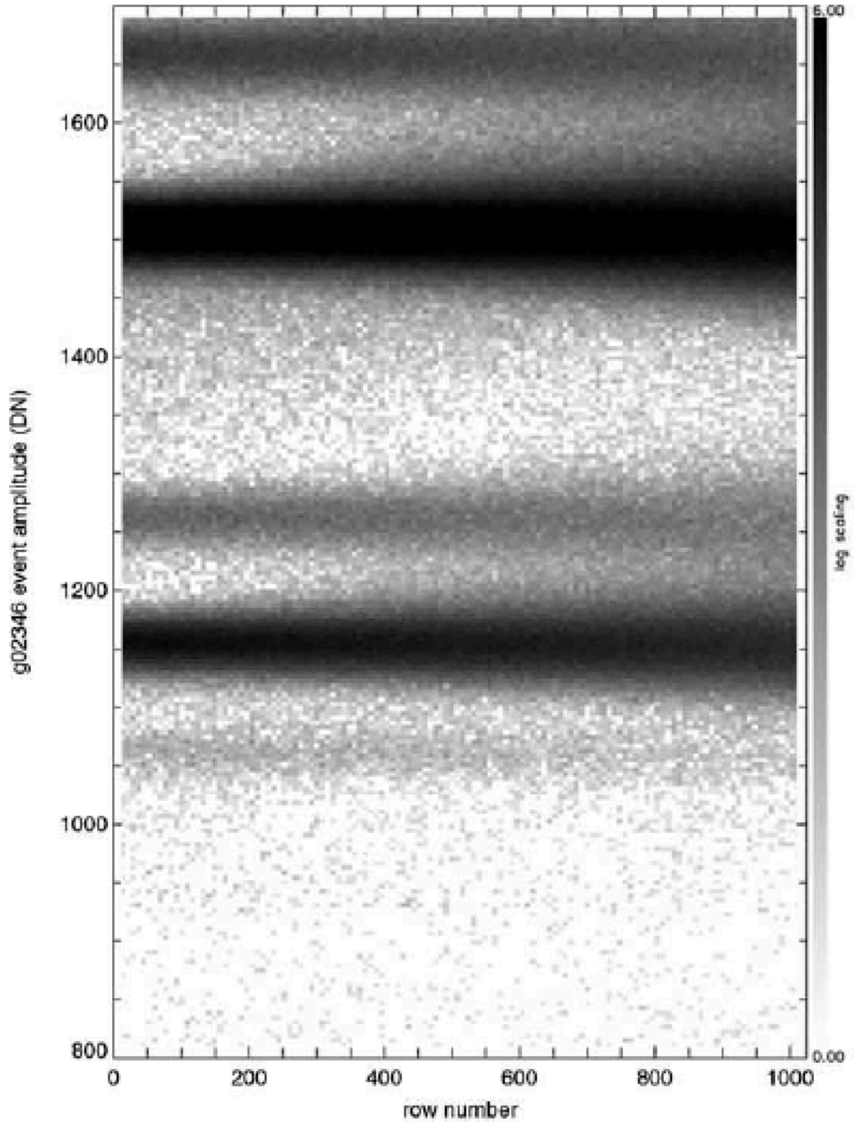

Charge Transfer Inefficiency

SNR 1E 0102.2-7219, standard calibration source with a soft, line-dominated spectrum.

Plucinsky et al. 2017, A&A, 597, 35.

I3: minimal CTI effects, low chipy

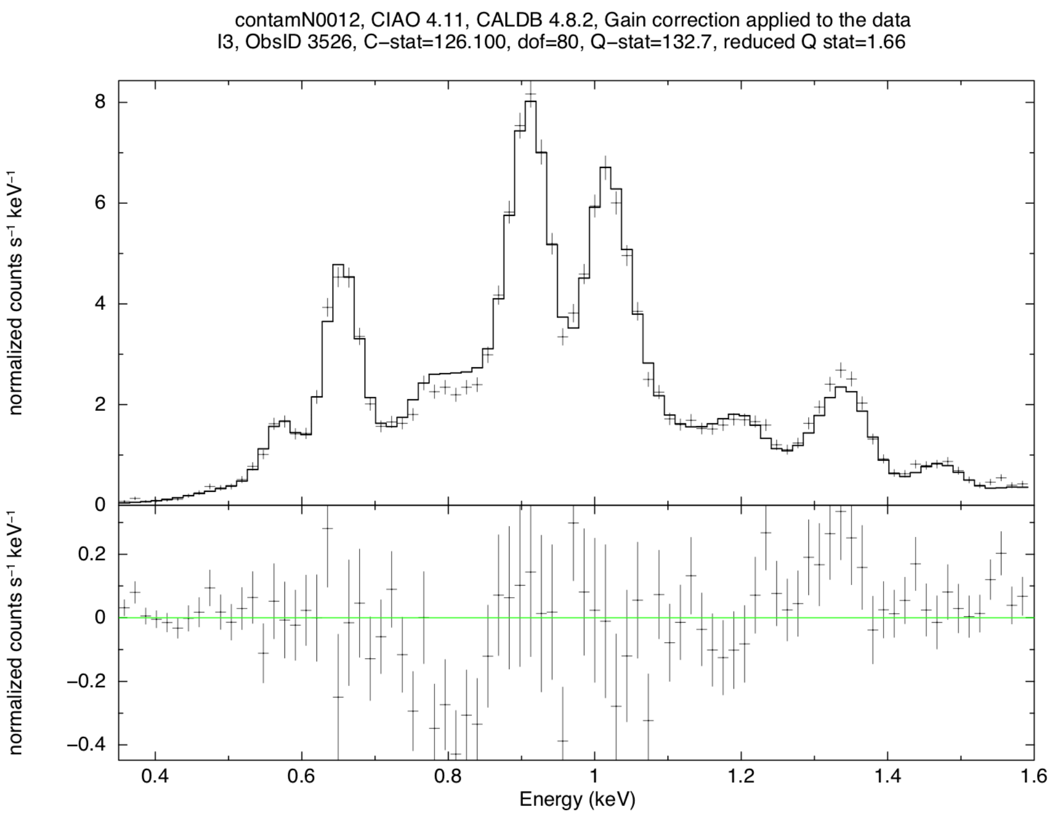

I3: maximal CTI effects, low chipy

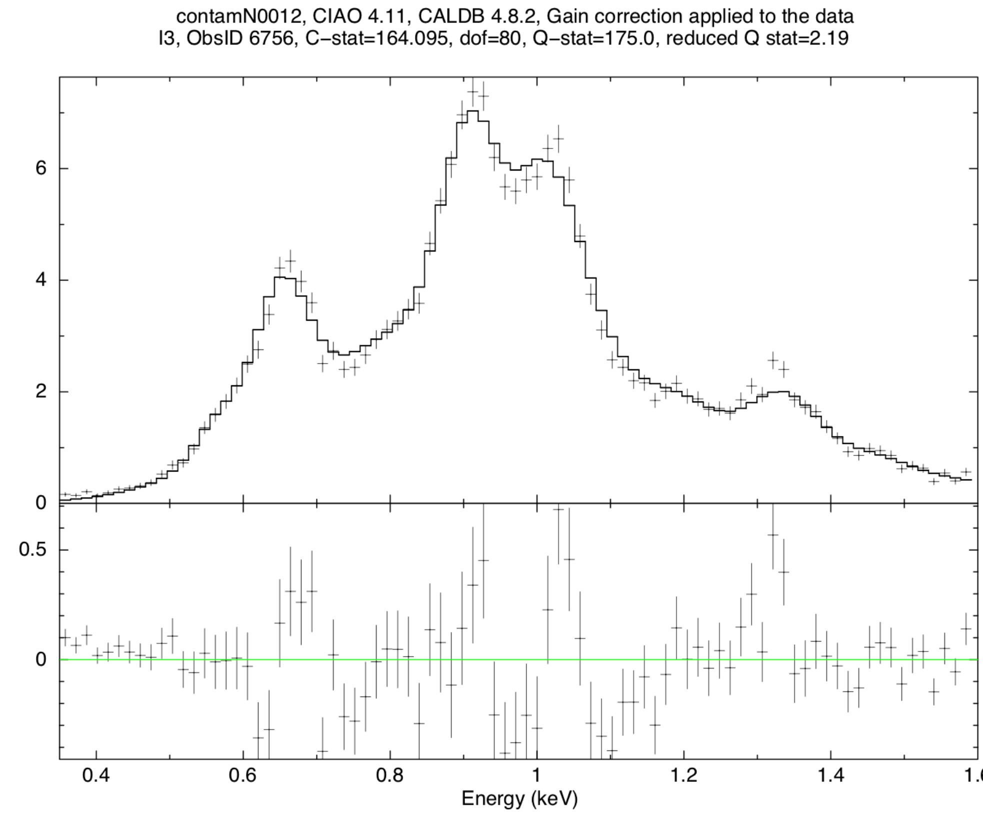

ACIS BI and FI Quantum Efficiency

The BI CCDs have higher QE over most of the bandpass than the FI CCDs. But the BI CCDs have higher background in the "accepted" grade set. For most GOs, the BI CCD is preferred but the FI CCDs are still the better choice for some observations.

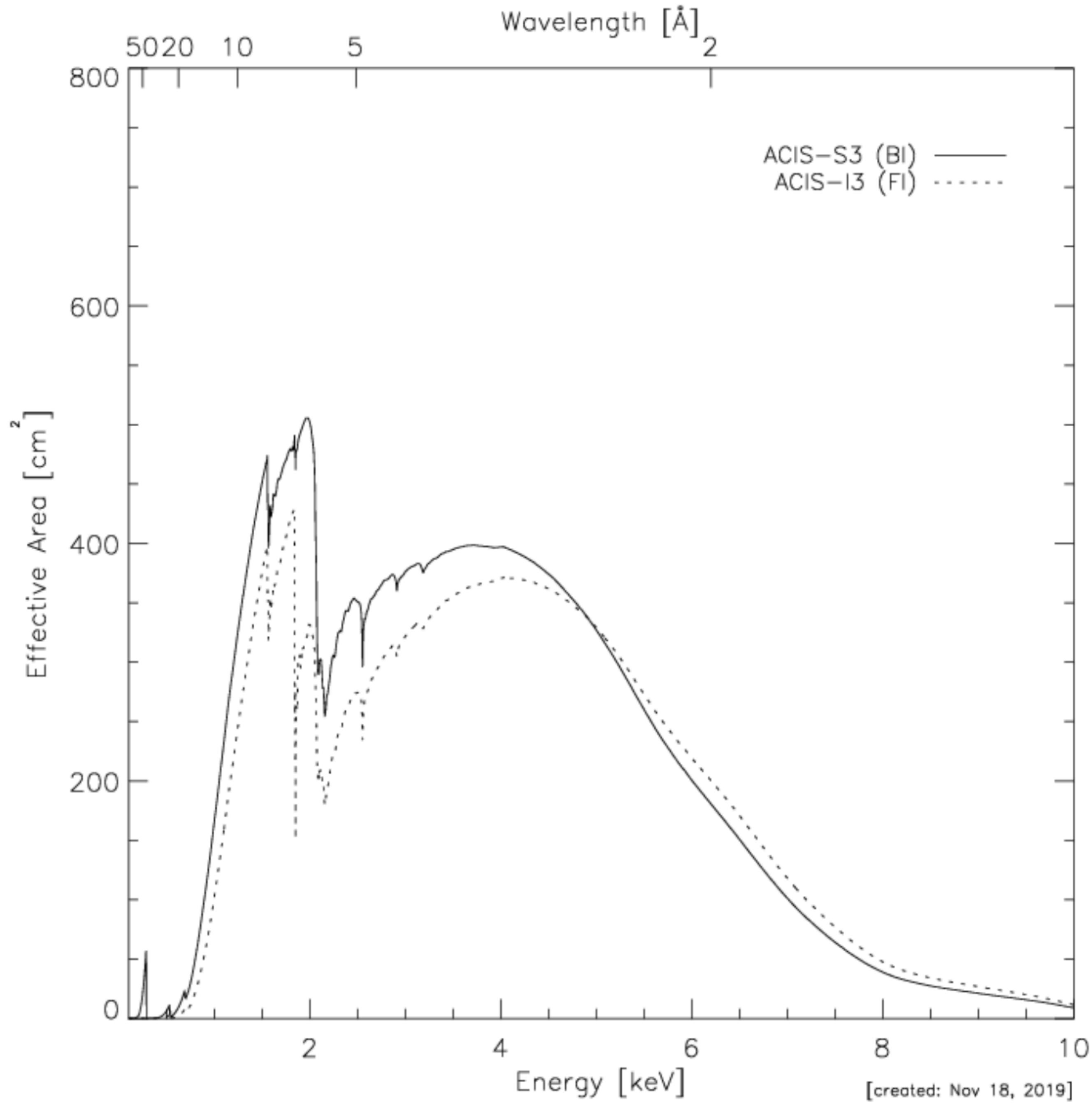

Reference on the physics of X-rays interacting with Si:

Fraser et al. 1994, NIM, 350, 368

Highly Recommended !!!!

Contamination

A layer of contamination has been building up on the ACIS Optical Blocking filter, reducing the effective area at low energies . Contaminant is mostly C, with some O and F.

Plucinsky et al. 2016,2018, 2020 SPIE.

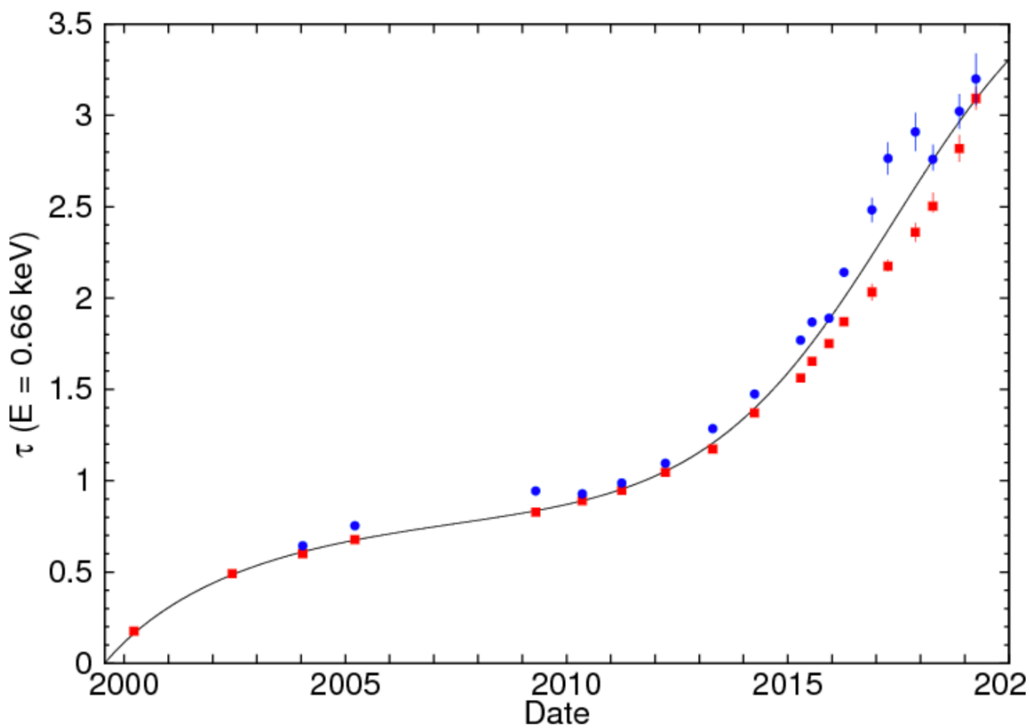

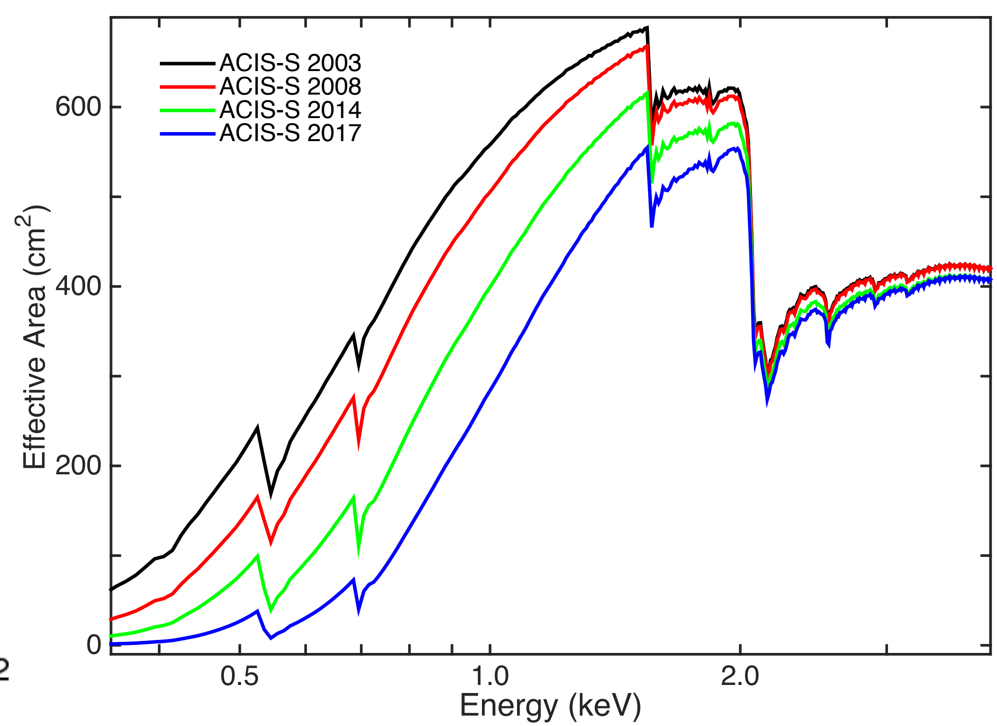

Contamination

SNR 1E 0102.2-7219, standard calibration source with a soft, line-dominated spectrum.

Plucinsky et al. 2017, A&A, 597, 35.

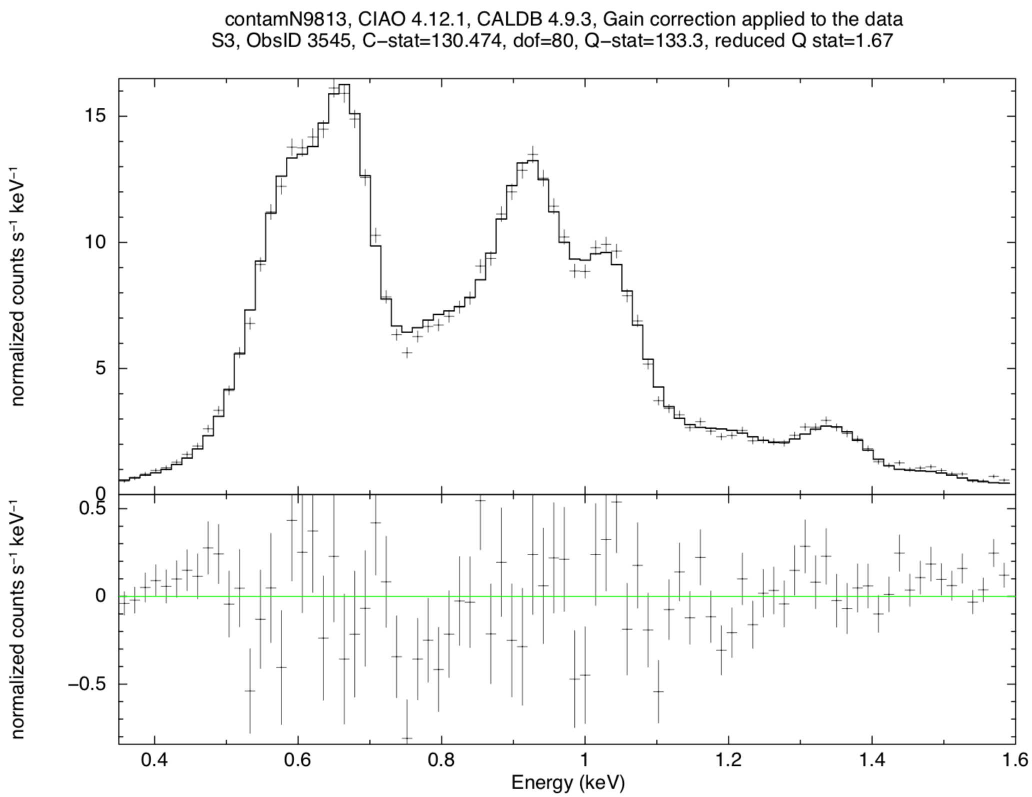

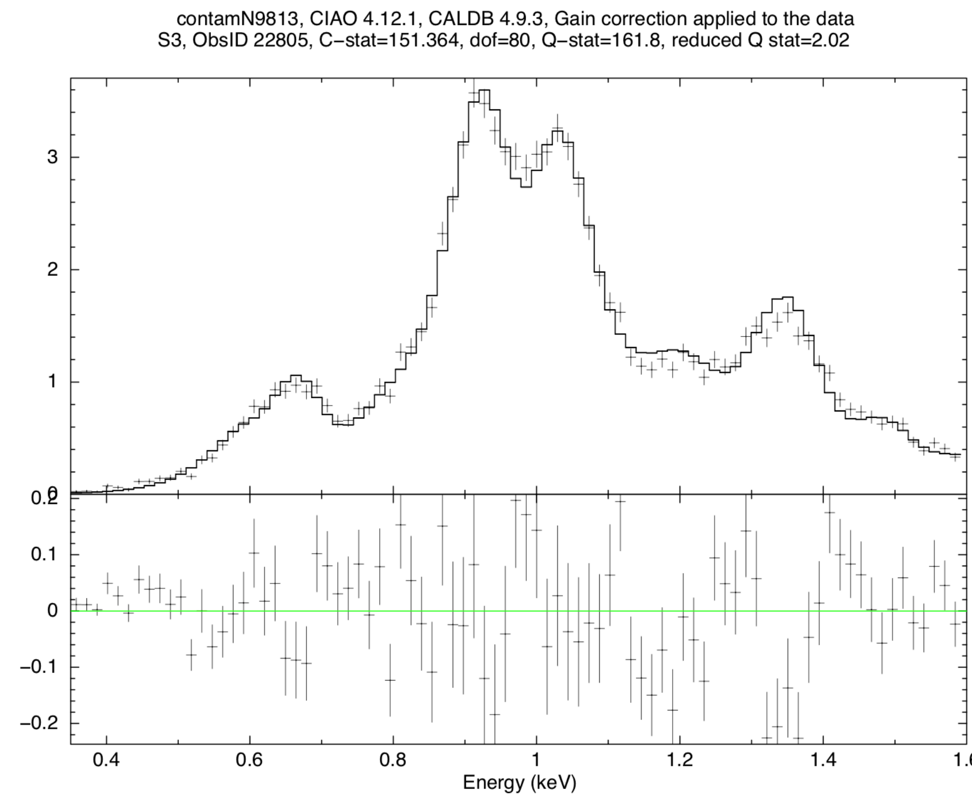

Stellar Birth and Life

Stars as They Form: Orion Nebula

Image credit: Matthew Spinelli

Stars as They Form: Orion Nebula

Stars as They Form: Orion Nebula

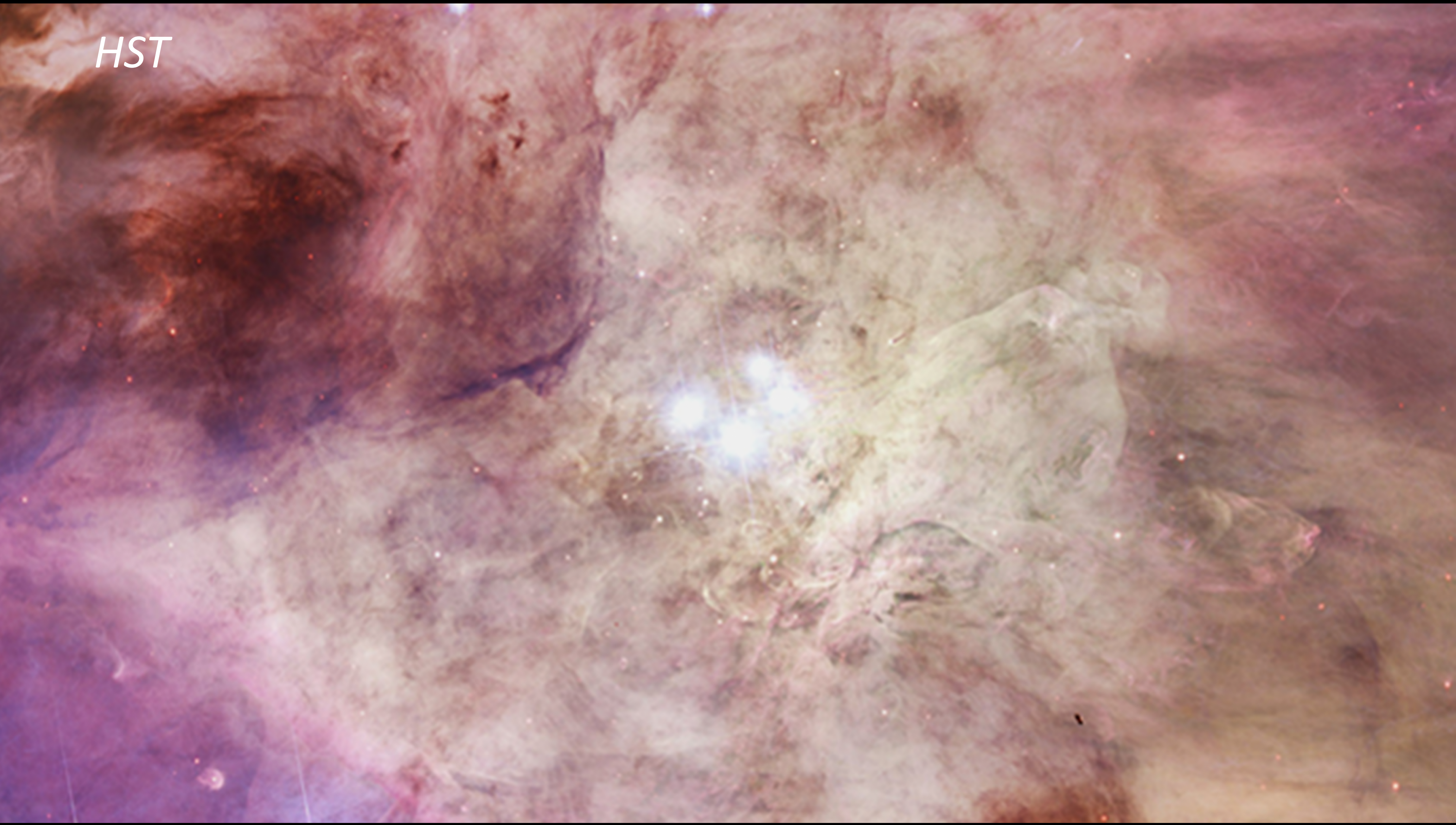

ROSAT Image of the Orion Nebula

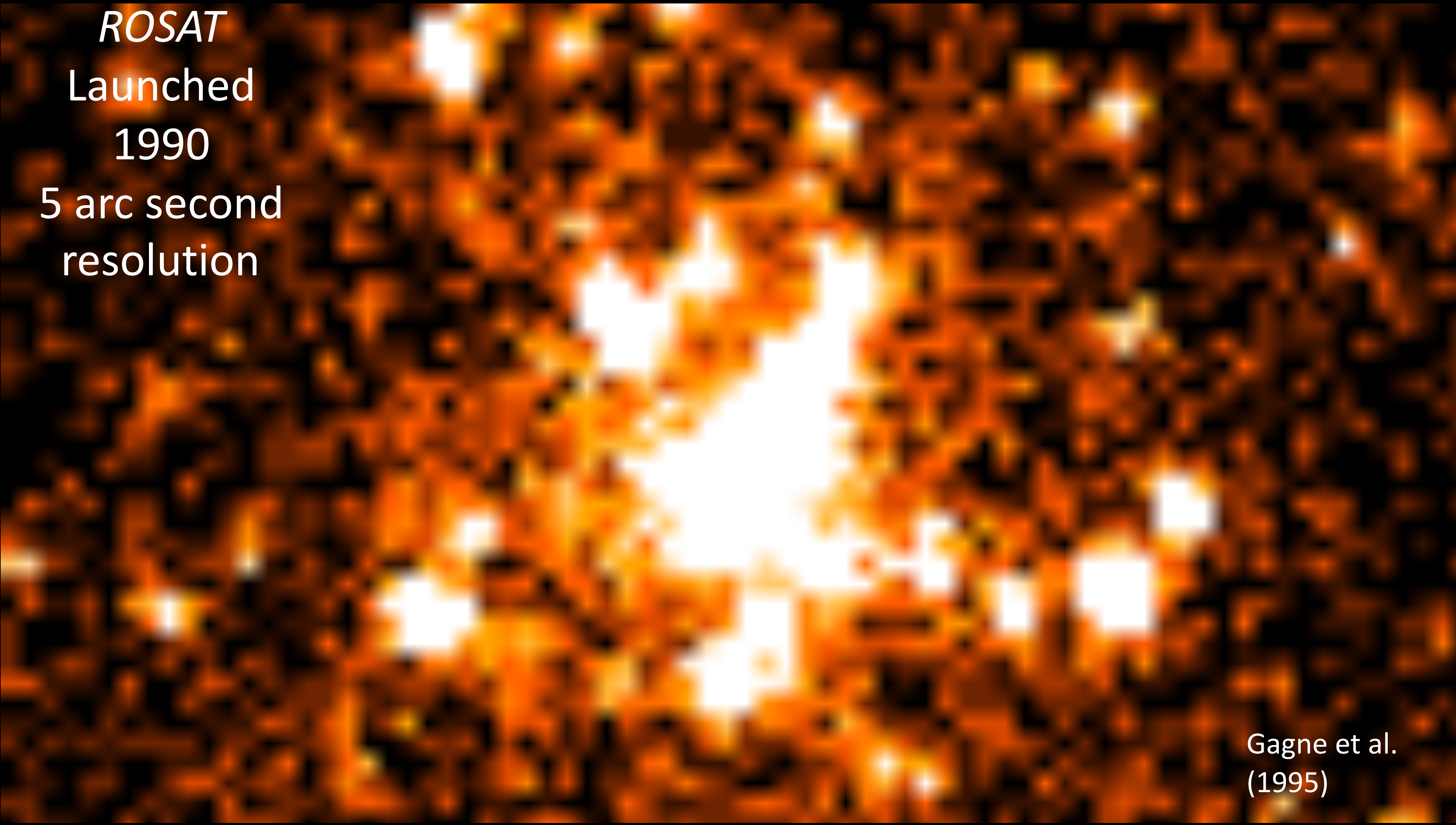

Chandra Image of the Orion Nebula

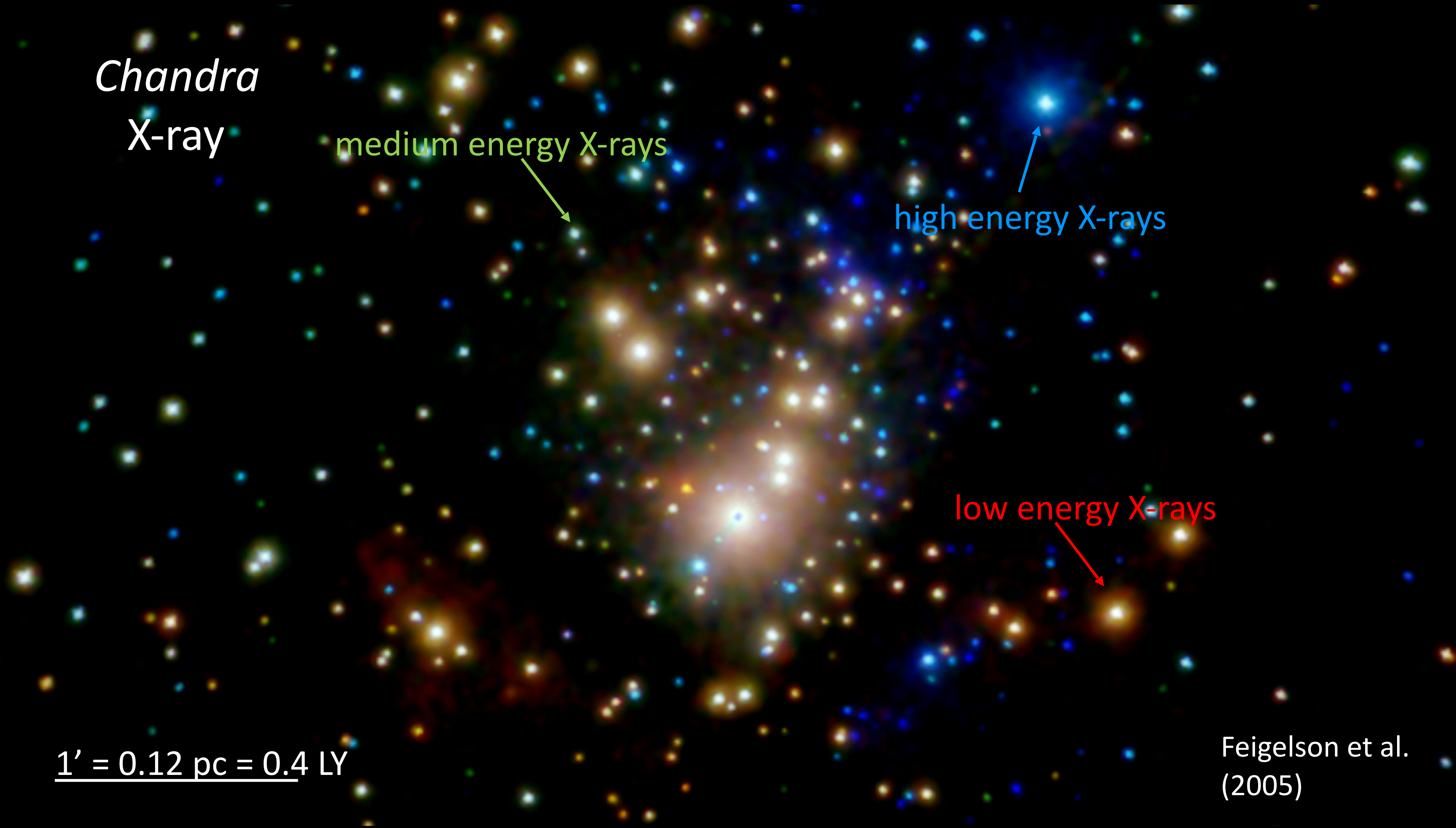

Channel Plate Detectors

Patnaude (CXC)

PHYSICAL PRINCIPLES

- High spatial and timing resolution/ low energy resolution
- consists of a stack of coated plates with micron sized pores
- An external electric field creates a voltage potential between two stacked plates
- When an X-ray impacts the plate, it creates a photoelectron which produces a cascade
- A wire grid detects the charge cloud and, based on the shape in both the X and Y axis, can precisely locate the position of the incident X-ray

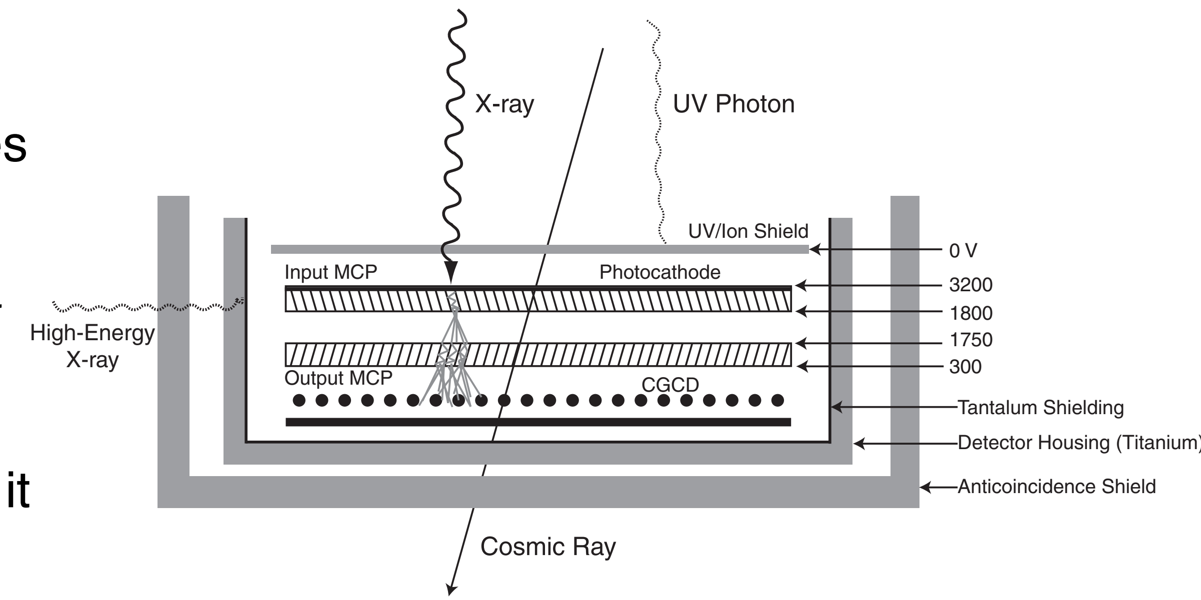

Cartoon representation of microchannel plate detector with anti-coincidence shielding

CHANDRA HIGH RESOLUTION CAMERA

Patnaude (CXC)

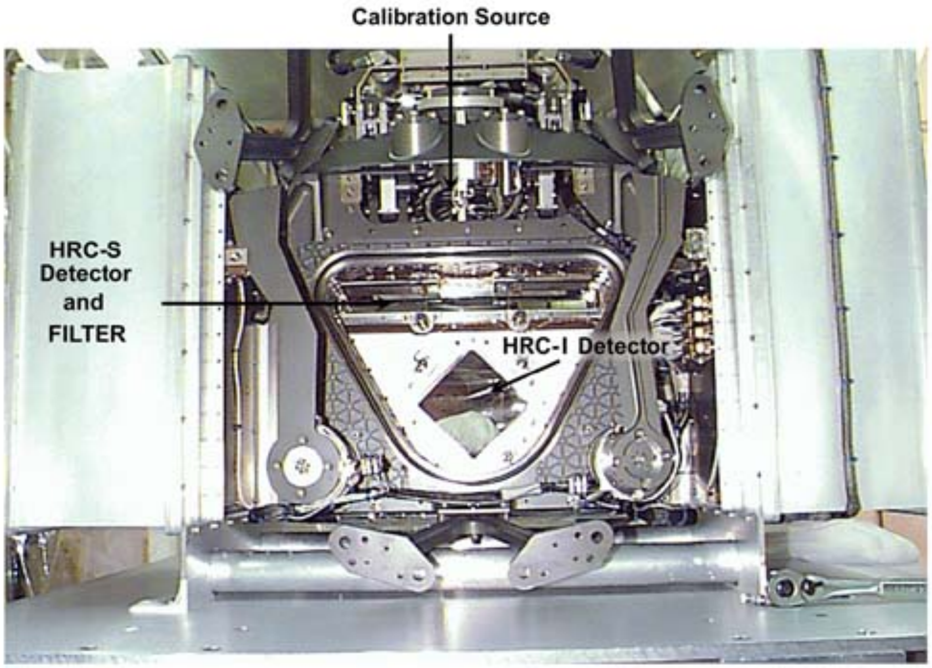

Looking into the HRC Vacuum Housing

The Chandra High Resolution Camera consists of a 30’ square imager (HRC-I) and an array of 10’ x 30’ plates which are tilted to roughly follow the Rowland Circle of the Low Energy Transmission Grating

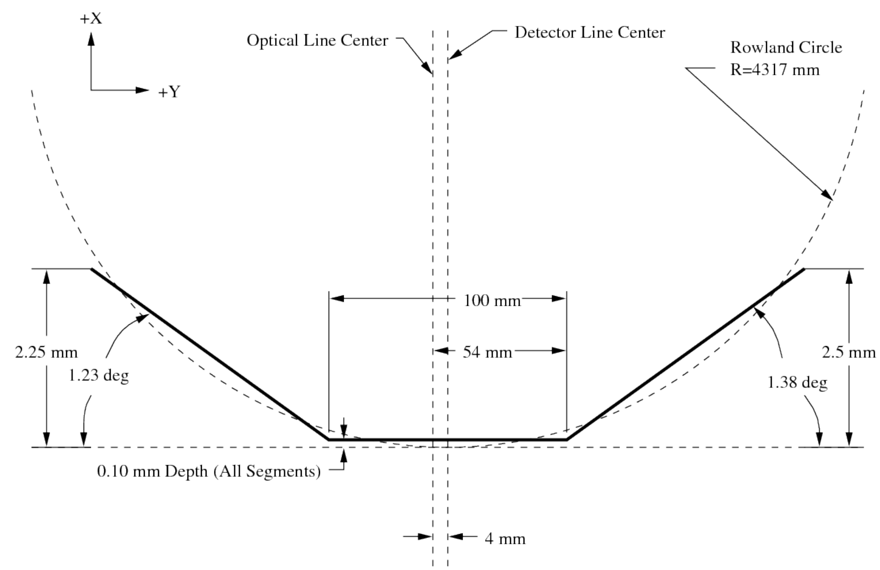

As initially configured, the HRC also included a set of shutter blades which could be positioned to block bright sources or the LETG 0th order image

High Resolution Camera Focal Plane Layout

Drake (CXC)

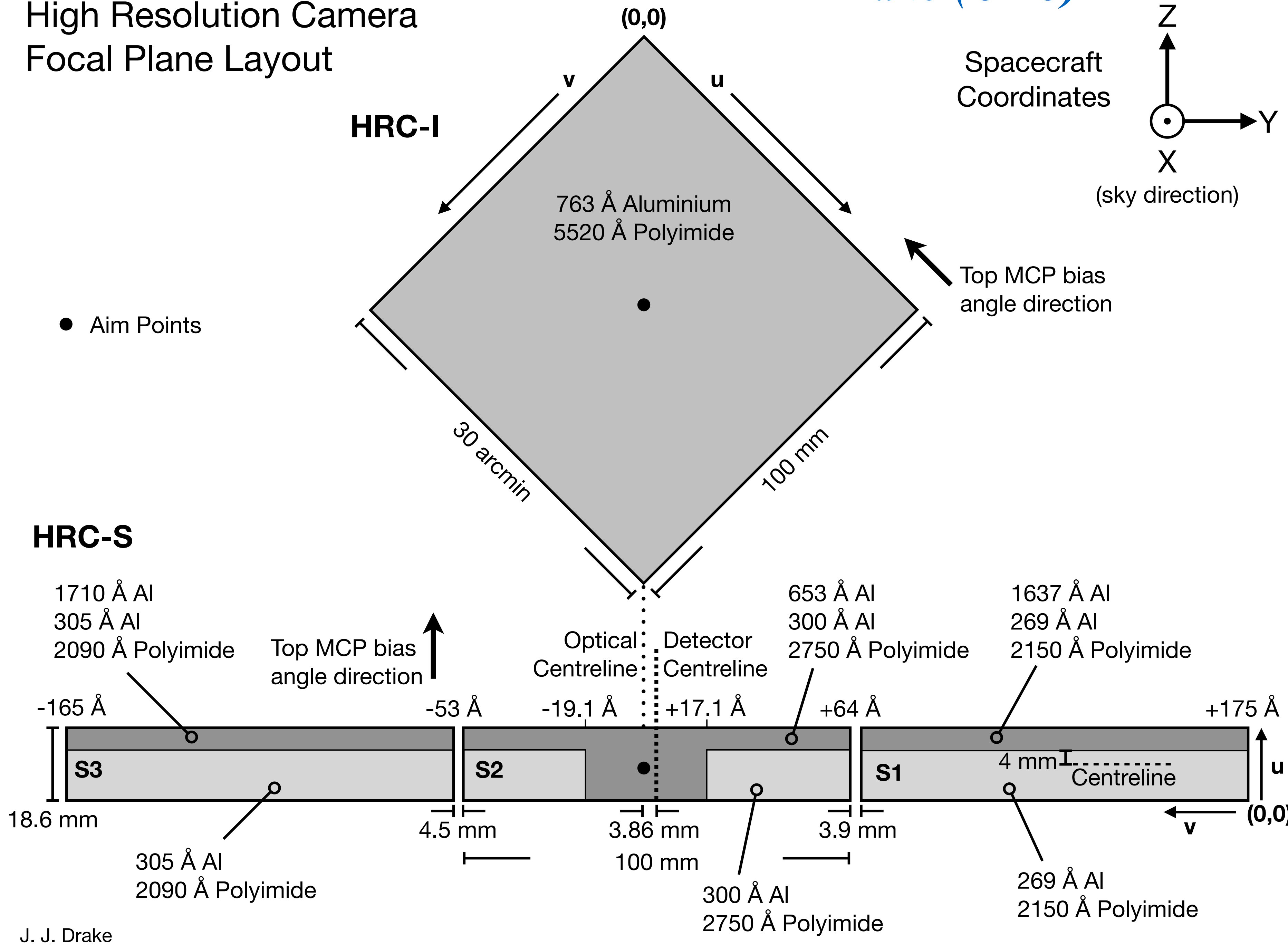

J. J. Drake

Patnaude (CXC)

Detector Characteristics

Focal-Plane Arrays		
HRC-I:	CsI-coated MCP pair	90 × 90 mm coated (93 × 93 mm open)
HRC-S:	CsI-coated MCPpairs	3-100 × 20 mm
Field of view	HRC-I:	∼ 30 × 30 arcmin
	HRC-S:	6 × 99 arcmin
MCP Bias angle:		6°
UV/Ion Shields:		
	HRC-I:	5520 Å Polyimide, 763 Å Al
	HRC-S:	
	Inner segment	2750 Å Polyimide, 307 Å Al
	Inner segment "T"	2750 Å Polyimide, 793 Å Al
	Outer segment	2090 Å Polyimide, 304 Å Al
	Outer segment (LESF)	2125 Å Polyimide, 1966 Å Al
Spatial resolution	FWHM	∼ 20μm, ∼ 0.4 arcsec
	HRC-I: pore size	10μm
	HRC-S: pore size	12.5μm
	HRC-I: pore spacing	12.5μm
	HRC-S: pore spacing	15μm
	pixel size (electronic read-out)	6.42938μm [0.13175 arcsec pixel^{-1}]
	pixel size (default binning size)	0.1318 arcsec pixel^{-1}
Energy range:		0.08 – 10.0 keV
Spectral resolution	$\Delta E/E$	∼ 1 @1keV
MCP Quantum efficiency		30% @ 1.0 keV
		10% @ 8.0 keV
On-Axis Effective Area:	HRC-I, @ .277 keV	133 cm^2
	HRC-I, @ 1 keV	227 cm^2
	HRC-S, @ .277 keV	97 cm^2
	HRC-S, @ 1 keV	224 cm^2
Time resolution		16 μsec (see Section 7.11)
Quiescent background in level 2 data	HRC-I	1.7×10^{-5} cts s^{-1} arcsec^{-2}
	HRC-S	6.3×10^{-5} cts s^{-1} arcsec^{-2}
Intrinsic dead time		50 μs
Constraints:	telemetry limit	184 cts s^{-1}
	maximum counts per aimpoint source	450000 cts
	linearity limit (on-axis point source)	
	HRC-I	∼ 5 cts s^{-1} (2 cts s^{-1} pore^{-1})
	HRC-S	∼ 25 cts s^{-1} (10 cts s^{-1} pore^{-1})

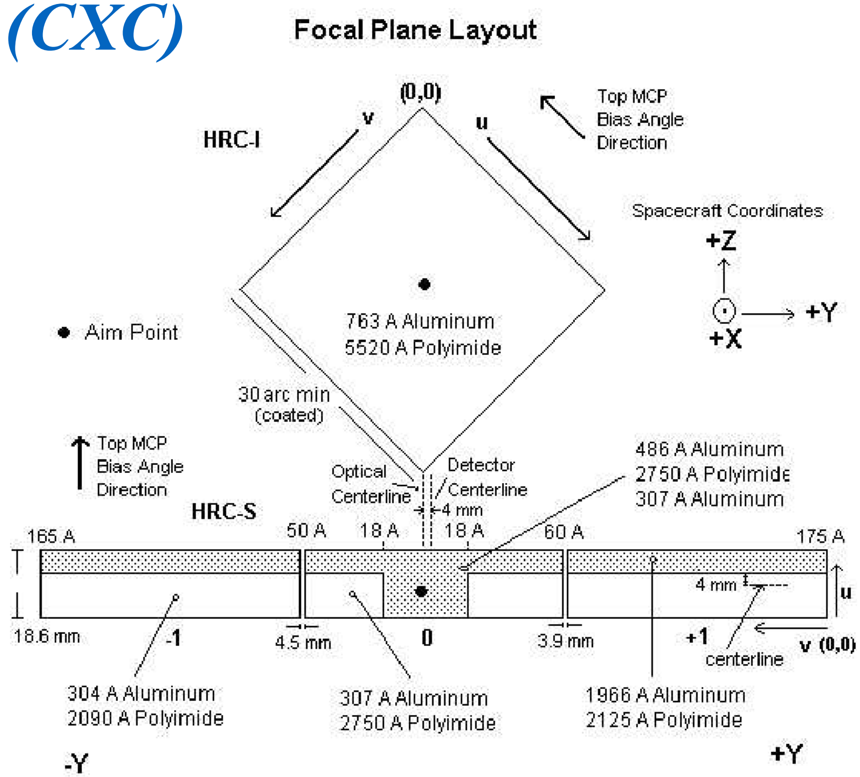

HRC (I and S) effective area is a convolution of the HRMA effective area, the transmission of the UV/Ion shield, and the quantum efficiency of the detector photocathode. As of 2020, the HRC area below 1 keV far exceeds that of ACIS

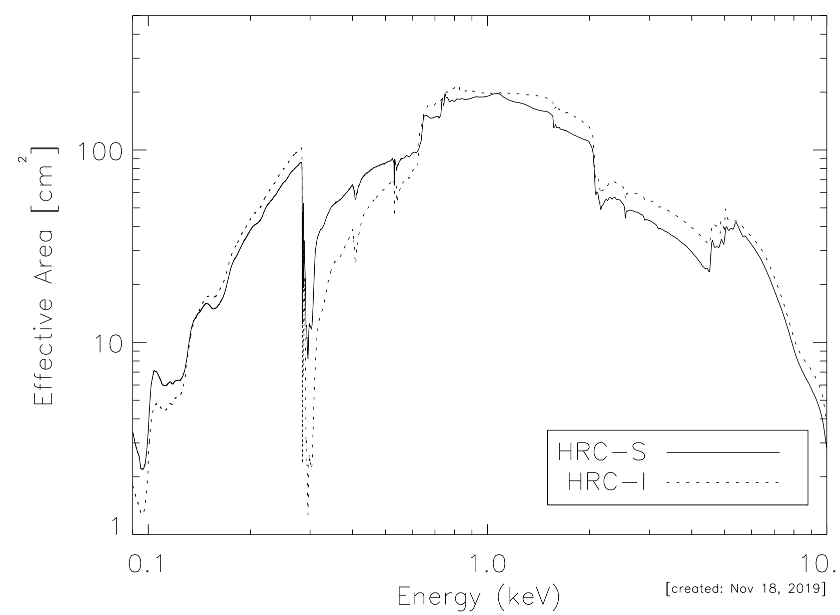

POSITION LOGIC

Patnaude (CXC)

- the charge cloud from the MCP stack is read out via a set of 64 hybrid preamplifiers
- the position of an X-ray event is determined by first determining the coarse position (from the strongest signal) and then computing a fine position correction by looking at the signal from adjacent amplifiers
- the same preamplifiers are used on both the imager and spectroscopy array
  - in the case of the spectroscopy array, additional logic is applied to each event in order to determine which plate the event landed on

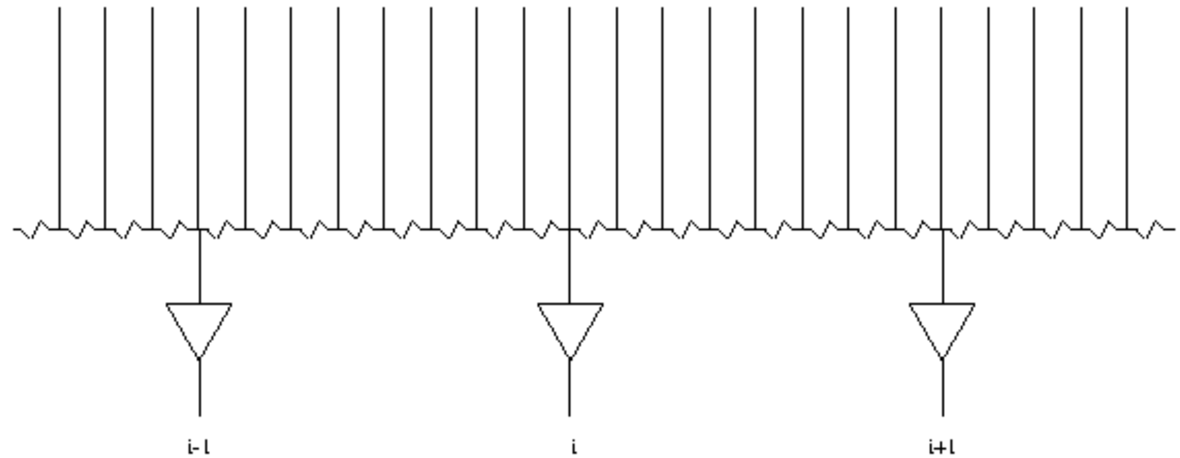

$$X_{fine} = \frac{A_{i+1} - A_{i-1}}{A_{i-1} + A_i + A_{i+1}}$$

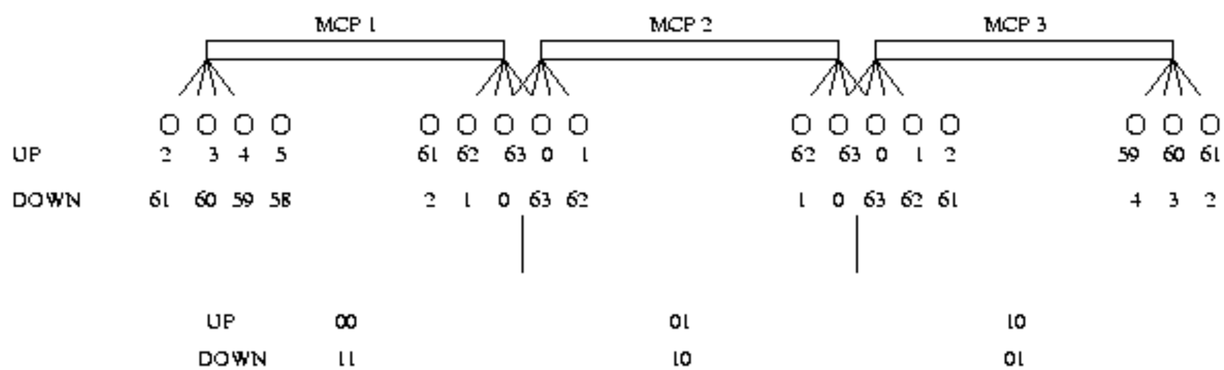

EVENT PROCESSING

Patnaude (CXC)

- The HRC reports both a valid event rate (up to 184 c/s while in observing mode, and 2 c/s when ACIS is in the focal plane and the HRC HV is up) and a total event rate
- The HRC is surrounded by a scintillator (anti-coincidence shield) which detects energetic particles which can also trigger event processing
- On board electronics can veto events which coincide with events detected by the anti-co shield
- In certain configurations, events can be properly time-tagged to do high precision timing measurements (the default configuration prohibits this, due to a wiring error which mis-tags events at the science data processor level in the electronics)

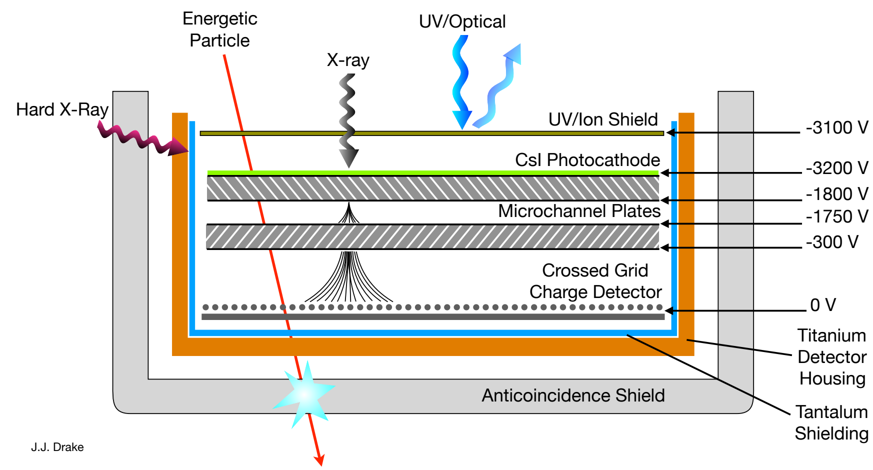

High Energy and Low Energy Transmission Gratings

Kashyap (CXC)

1. THEORY

BRAGGING ON THE X-WAVES

$$n\lambda = 2d \sin\theta$$

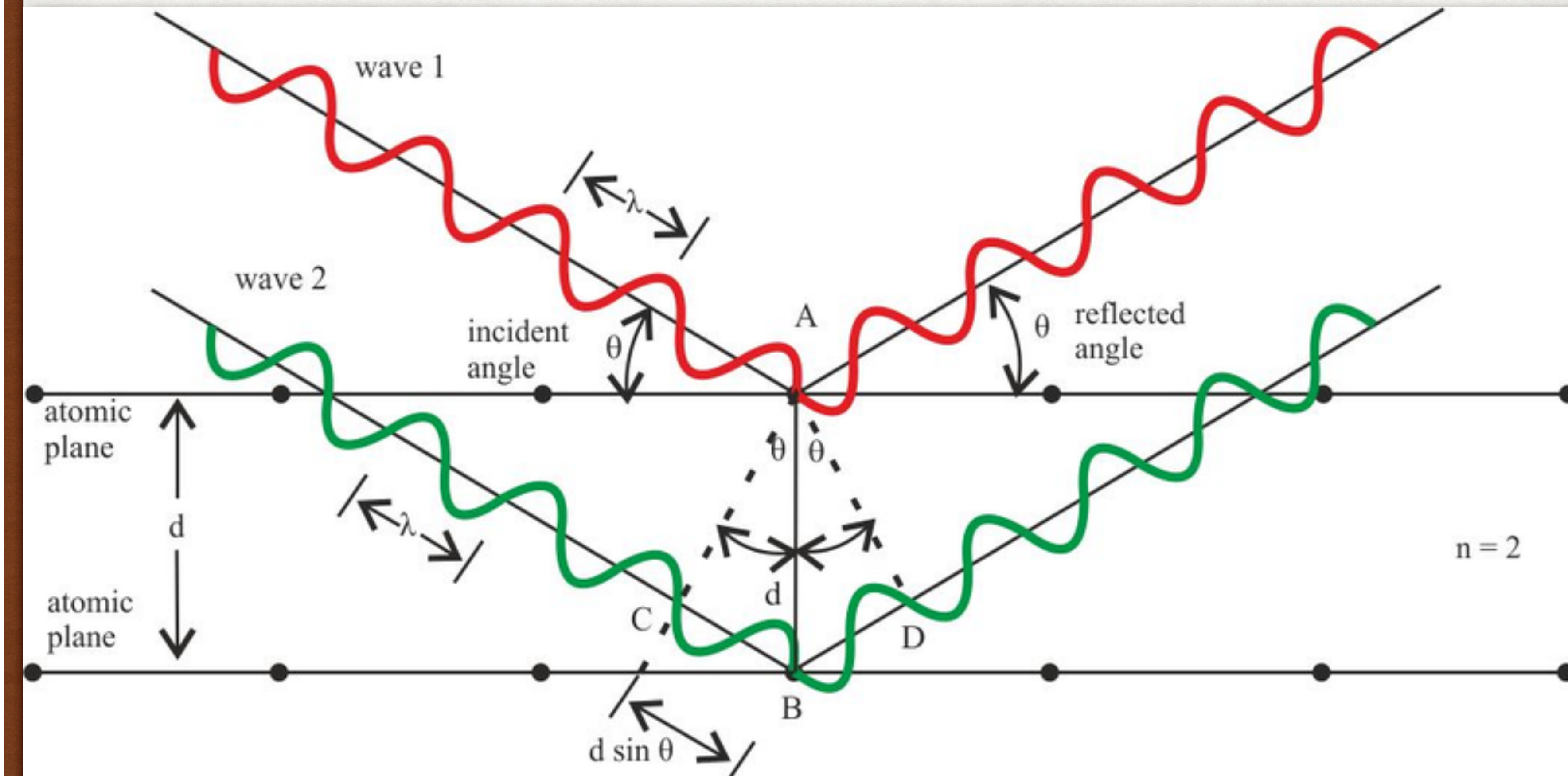

vlk: CIAO Workshop AS235/Honolulu 2020 Jan 3-4

Naemi Waeselmann (researchgate)

Kashyap (CXC)

1. THEORY

ROWLAND CIRCLE

small angles; YY' assumed negligible

Concave reflection grating
radius=2×Rowland

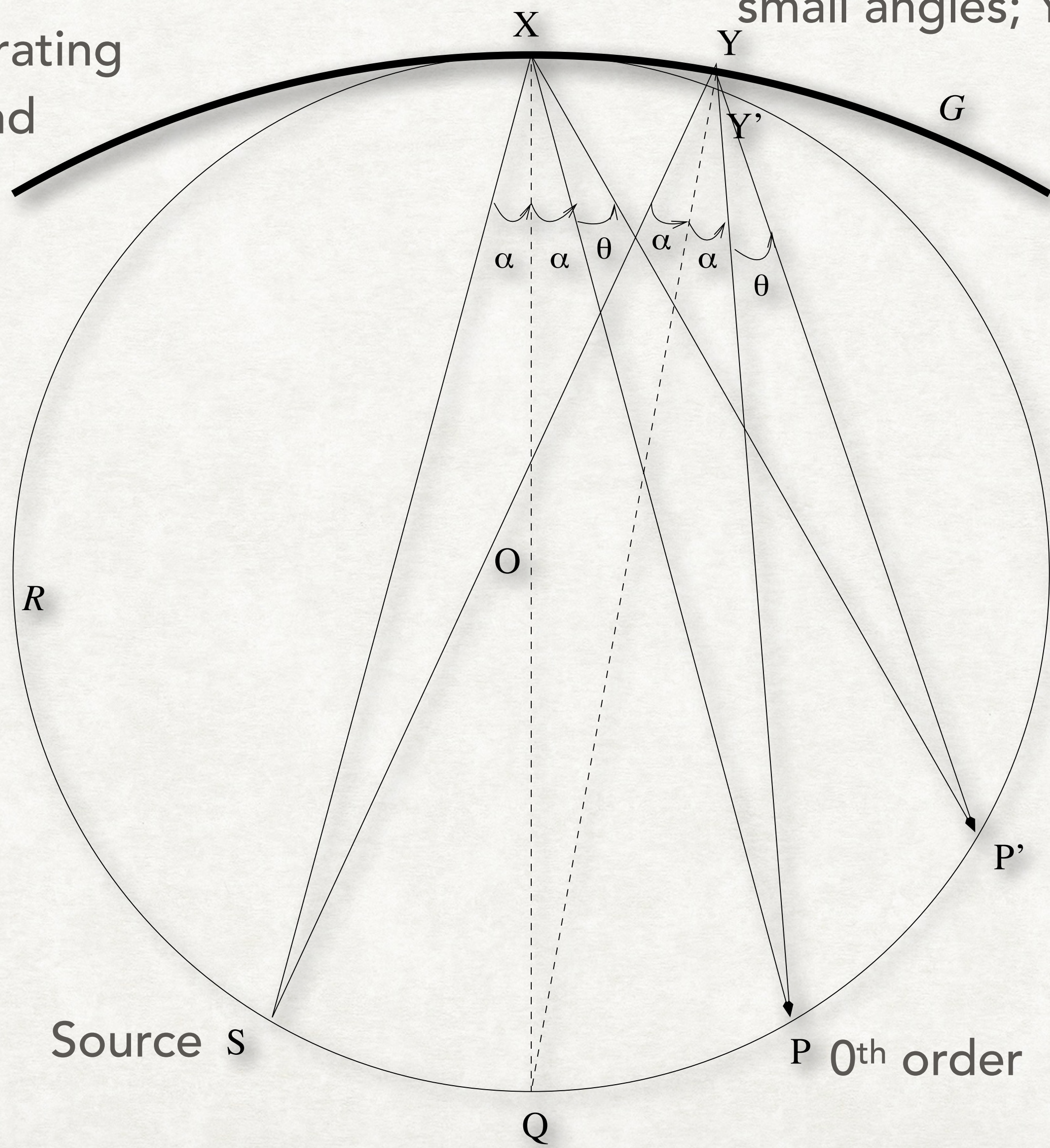

Rowland circle

dispersed $\theta \propto \lambda$

Source

0^{th} order

Kashyap (CXC)

1. THEORY

TRANSMISSION GRATING GEOMETRY

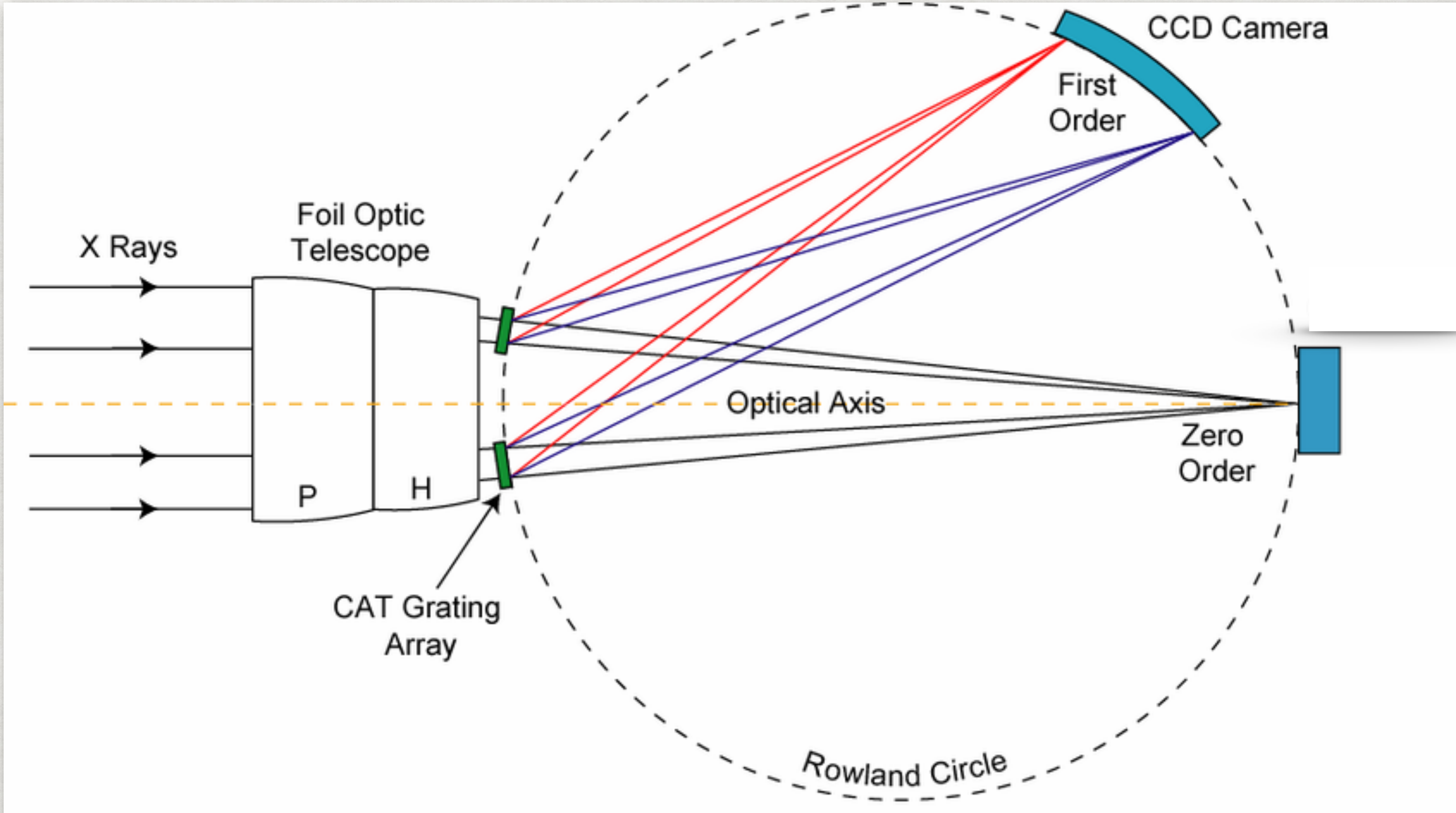

Flanagan et al. 2007, Proc.SPIE 6688, 66880Y

Kashyap (CXC)

1. THEORY

ORDERS AND DISPERSION RELATION

- You can measure the distance of a photon from the zeroth order in the detector plane and translate that distance to $n\lambda$
- If there is enough intrinsic energy resolution in the detector, you can separate the orders and remove the degeneracy in λ
- In the small angle approximation at which most gratings operate, distance along the detector,

  $\textit{dispersion distance} \propto \delta\theta \propto \lambda$
- Resolution is limited by the size of the 0th order image, with

  $\delta\theta \propto \textit{PSF-width} \propto \delta\lambda$

  Along the Rowland circle, this is fixed, so

  $\delta\lambda \approx \textit{constant} \Rightarrow$ Resolution $\lambda/\delta\lambda\uparrow$ as $\lambda\uparrow$

2. HARDWARE

HETGS

- High-Energy Transmission Grating Spectrometer
  - Two gratings in one: Medium Energy Grating (MEG) for outer mirror shells, and High Energy Grating (HEG) for inner shells
- The facets are tilted (+4.7° MEG, –5.2° HEG), leading to two arms which intersect at the 0^{th} order
- The MEG period is ≈2× HEG's, so wavelength coverage of MEG is double that of HEG, with half the resolution
- Primary detector is ACIS-S, optionally also HRC-I (but as yet unsupported)
- Chandra POG Chapter 8:

  http://cxc.harvard.edu/proposer/POG/html/chap8.html

Kashyap (CXC)

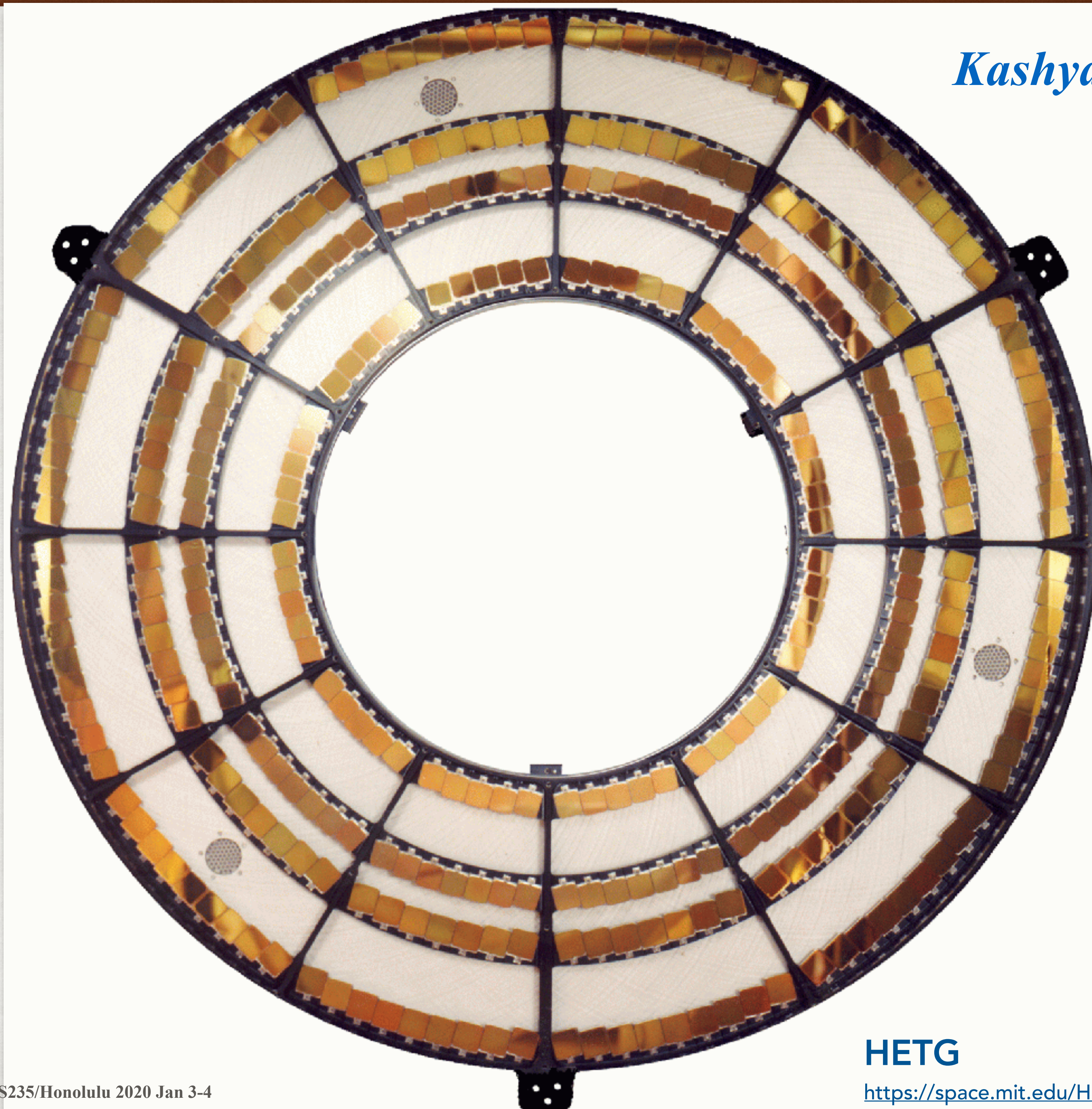

HETG

https://space.mit.edu/HETG/hetg_info.html

Kashyap (CXC)

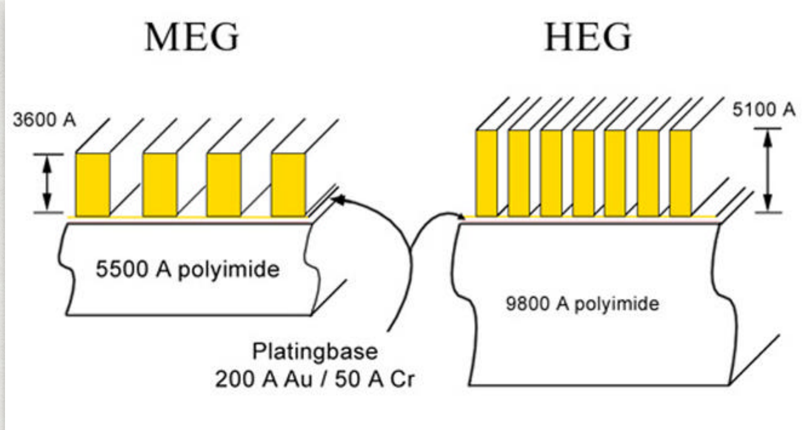

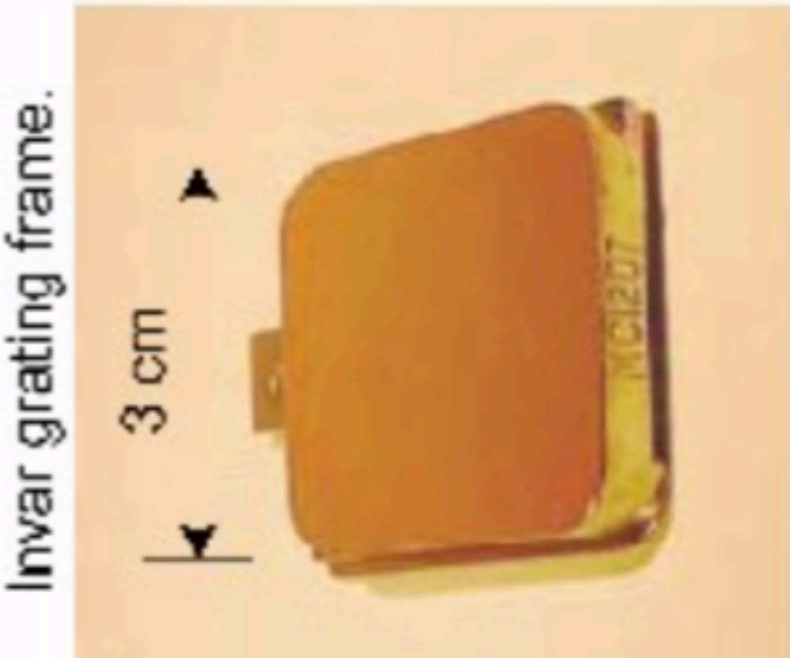

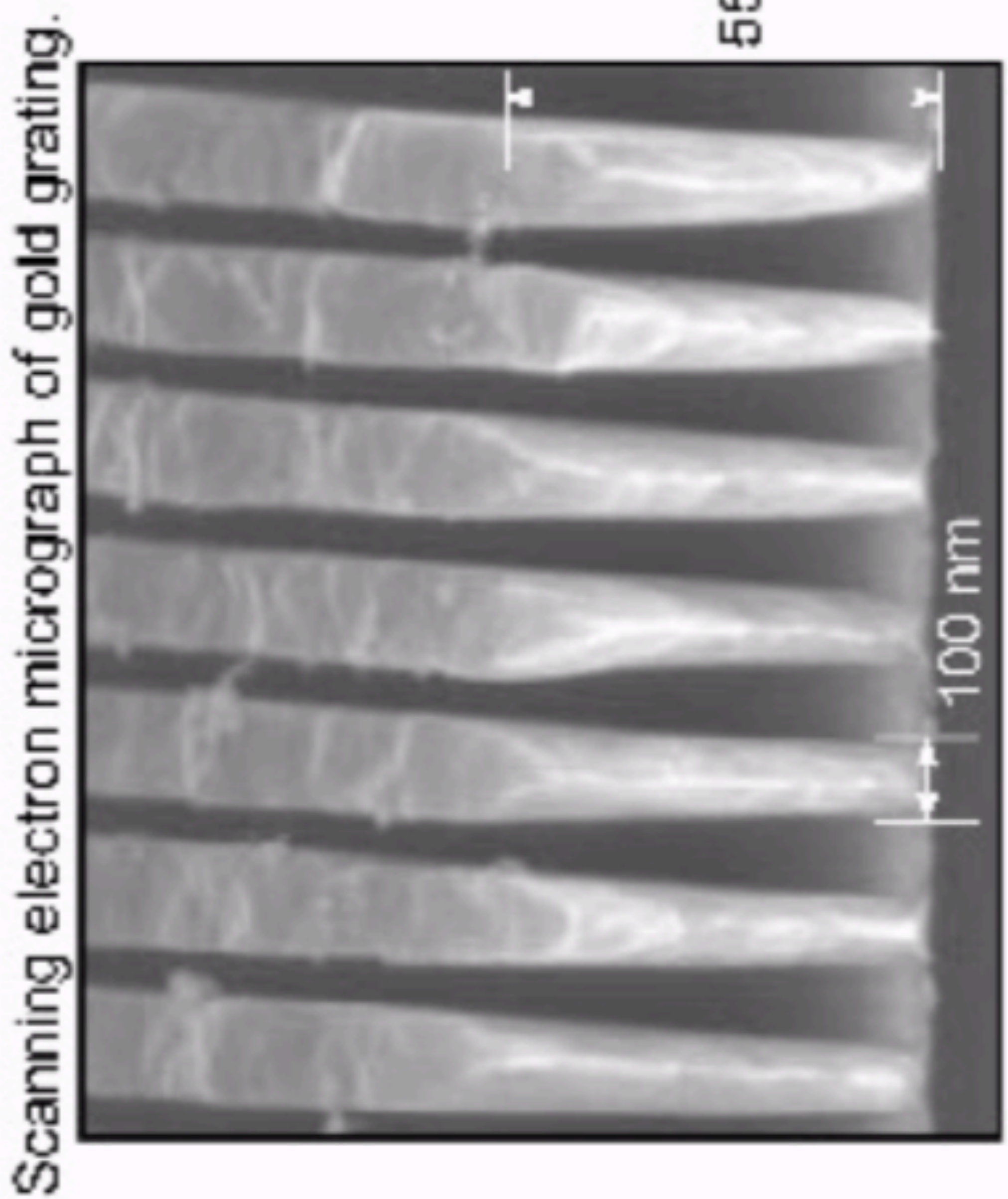

HETG facets and bars

https://space.mit.edu/HETG/hetg_info.html

(Mike Nowak)

HETGS schematic and footprint on ACIS-S

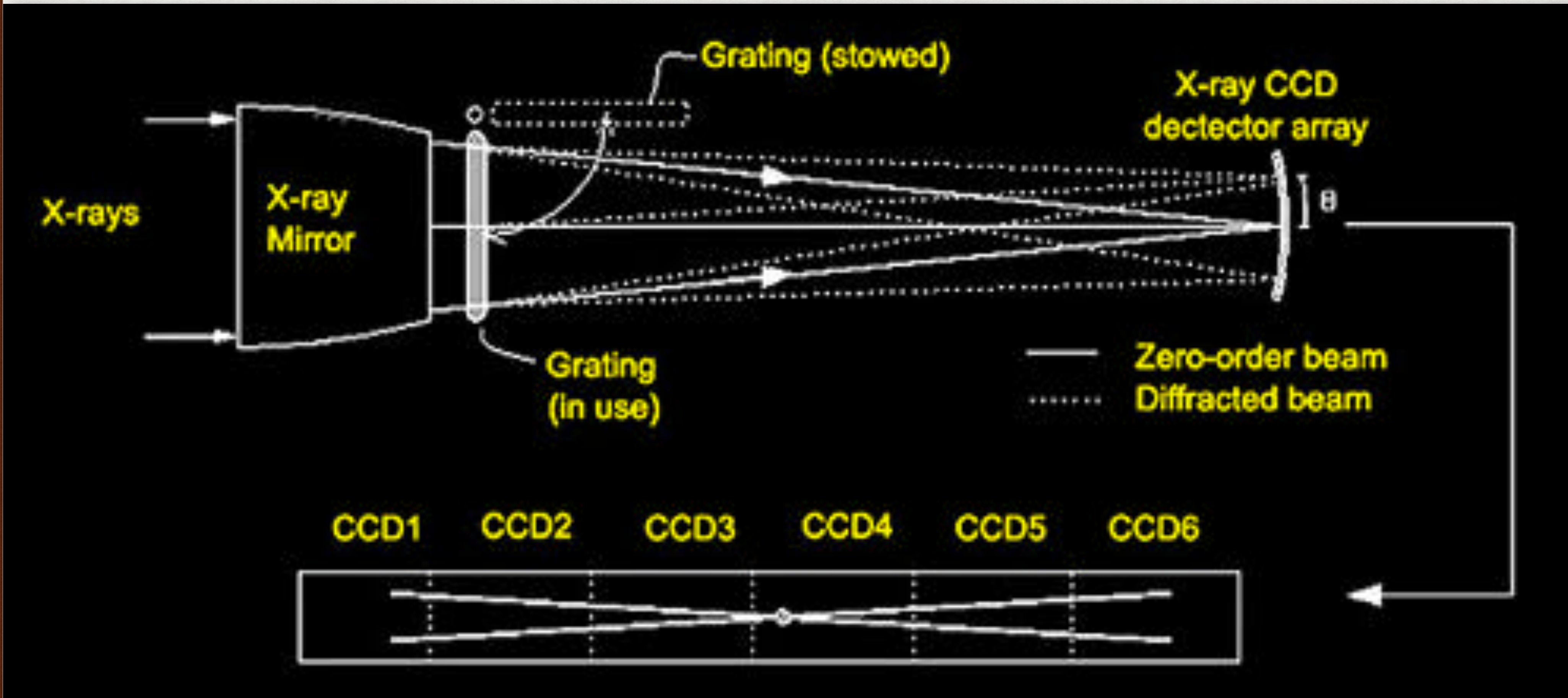

(chandra.harvard.edu)

Kashyap (CXC)

2. HARDWARE

HETGS+ACIS-S

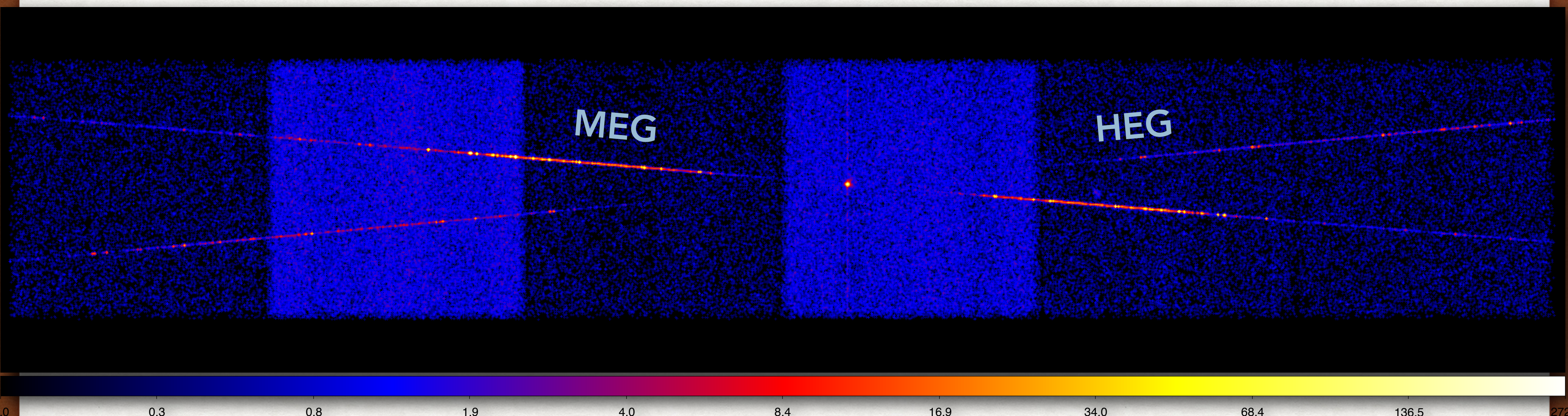

Capella ObsID 1235

Kashyap (CXC)

2. HARDWARE

LETGS+ACIS-S

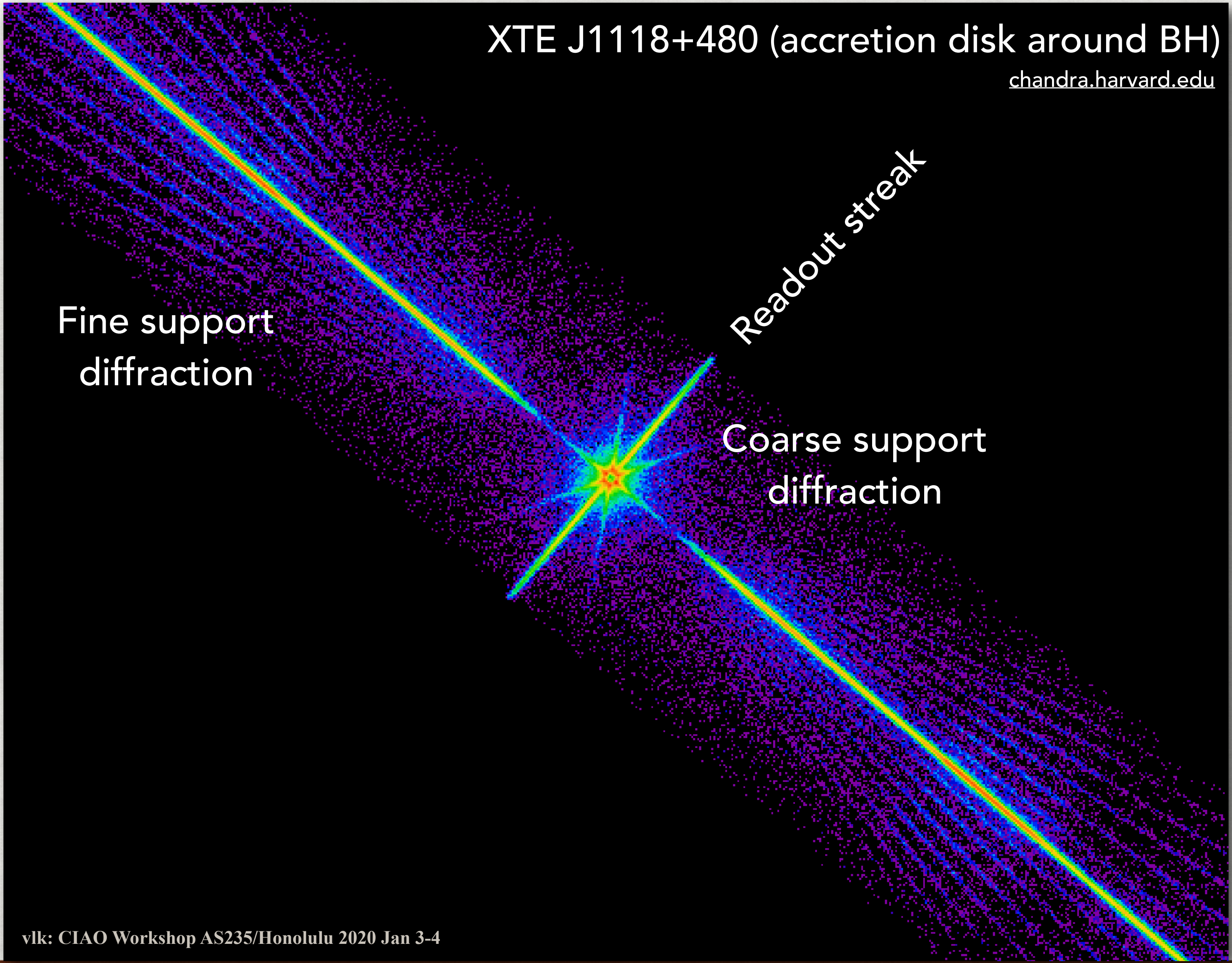

Science

Nowak (CXC)

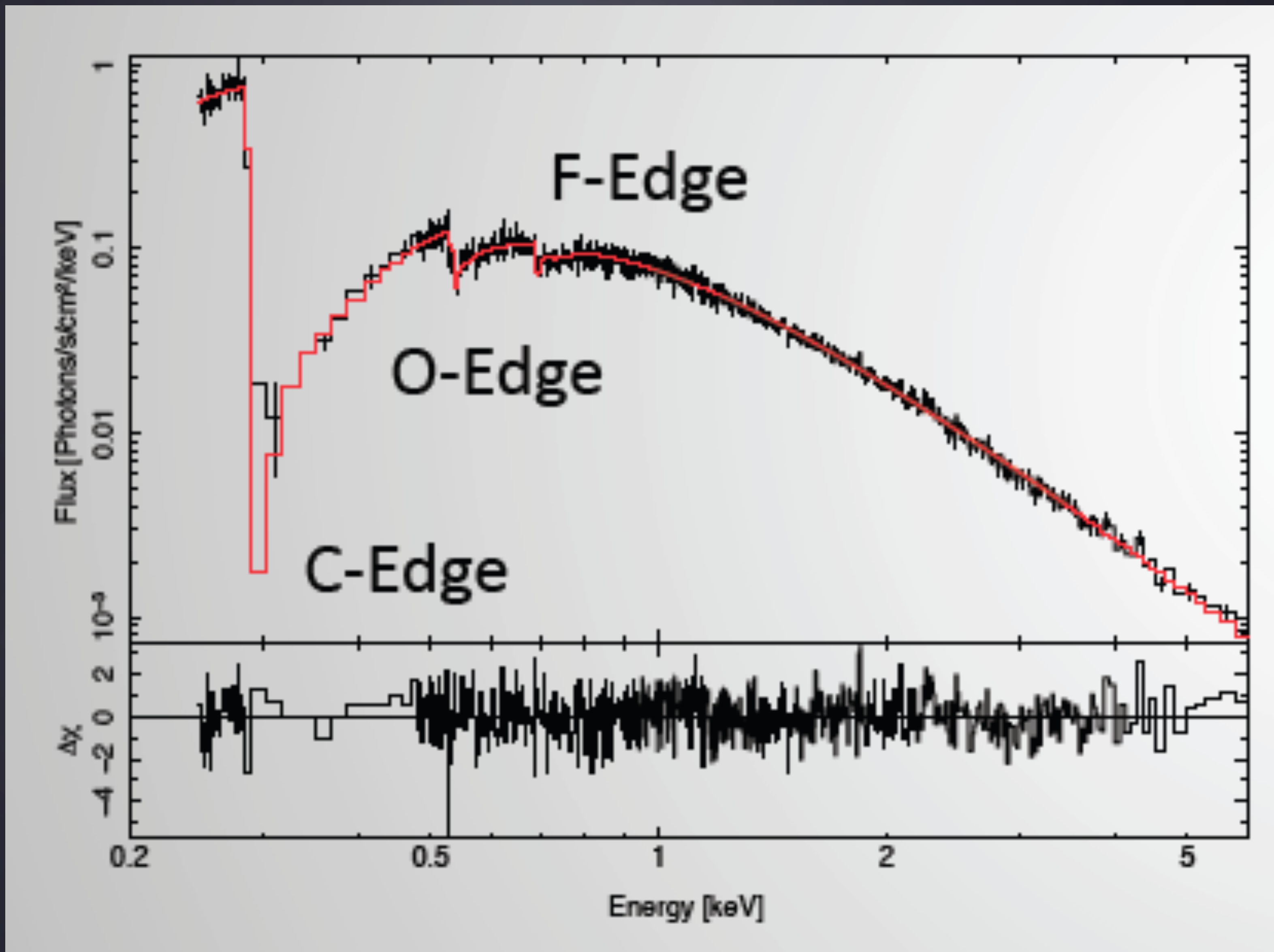

(H. Marshall)

Tracking Contaminant on Chandra-ACIS

Science

Nowak (CXC)

GX 301-2

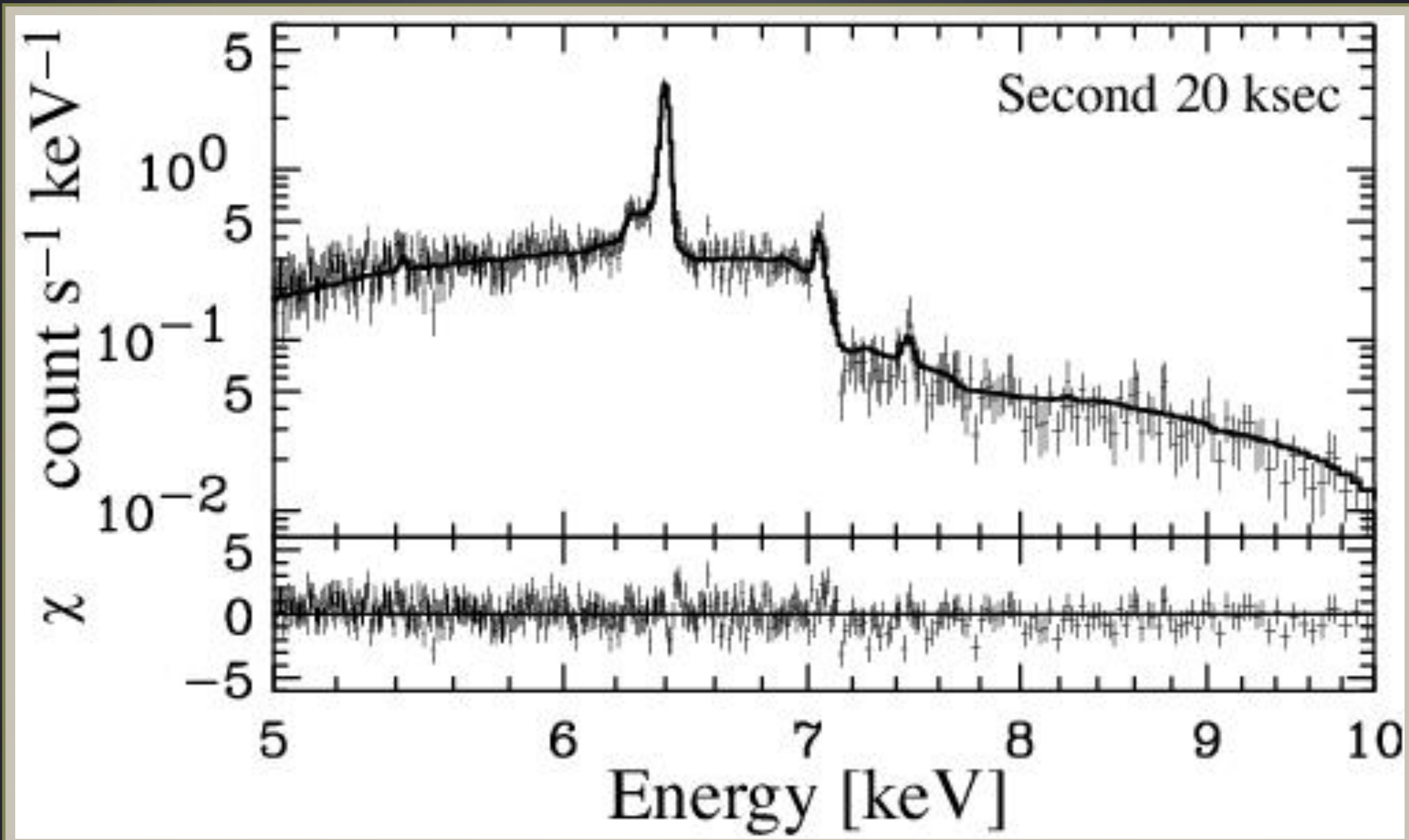

(Watanabe et al. 2004)

Science

Nowak (CXC)

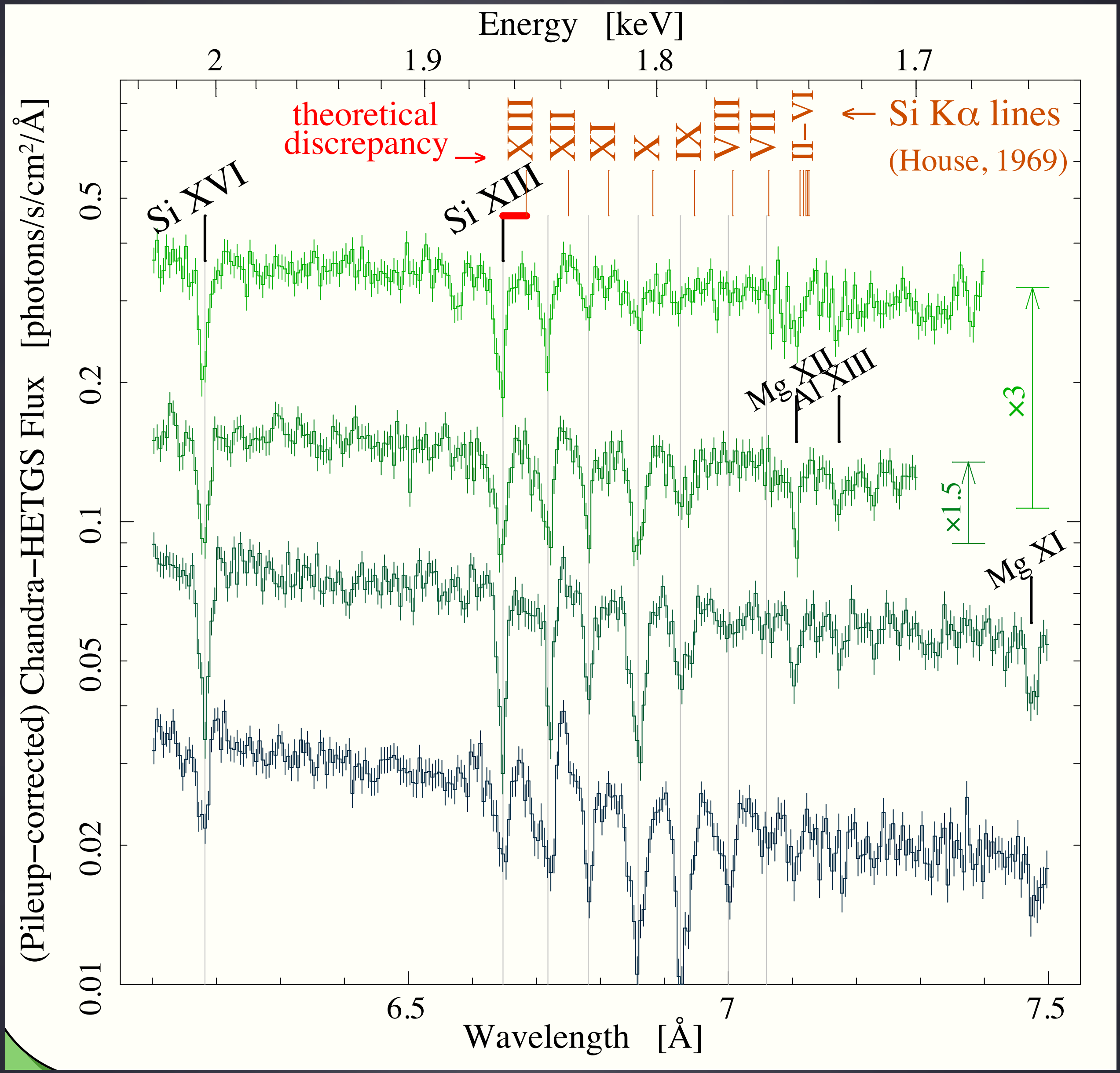

Stellar Winds (Cyg X-1 HMXB Wind)

Science

Nowak (CXC)

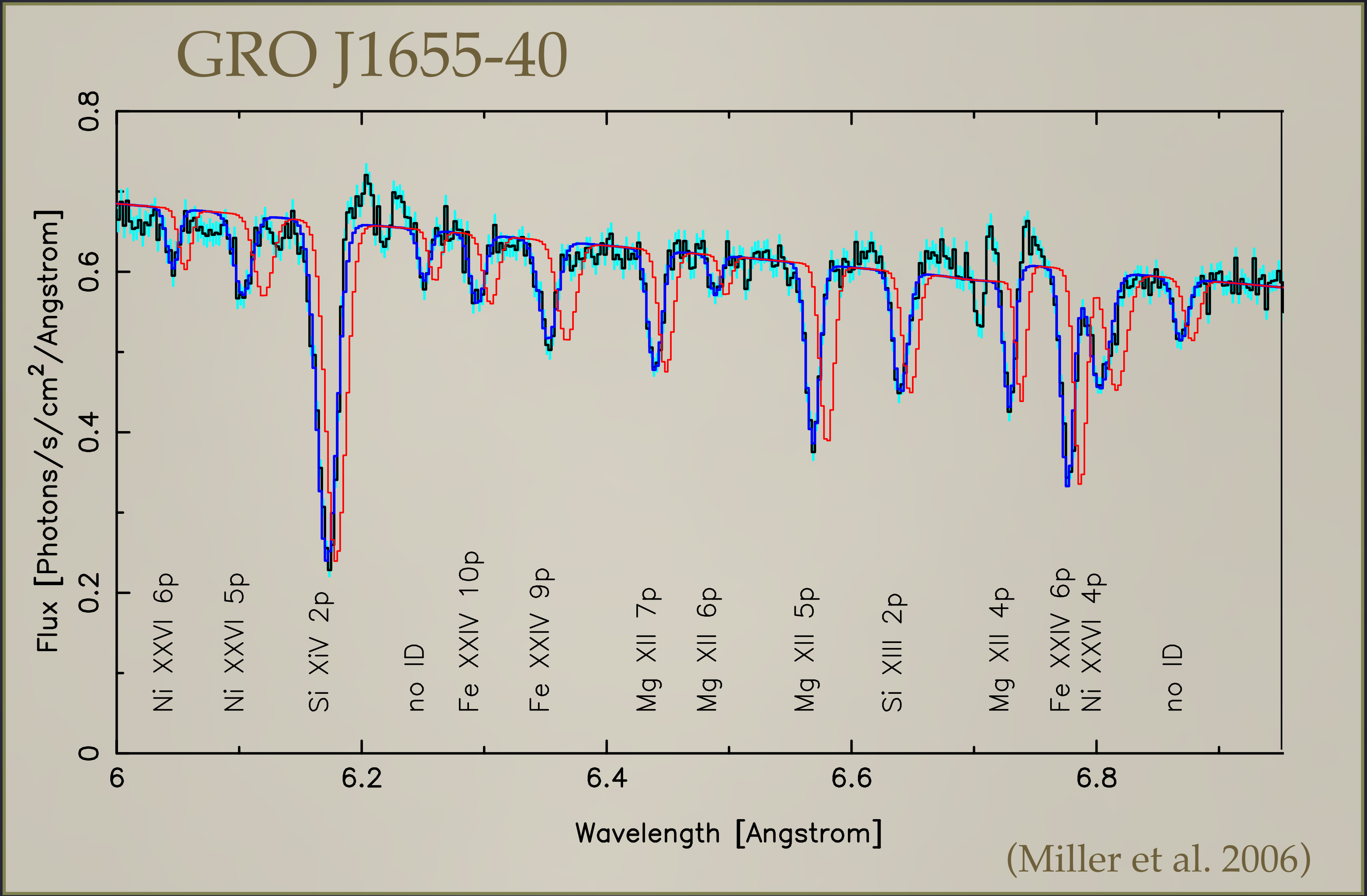

Magnetized Accretion Disk Winds

Summary

Chandra continues to produce spectacular results even as the science instrument have suffered some degradation in flight.

Even though the satellite is 21 years old, there are no life-limiting items that would prevent operations for another 10 years.

Chandra is a NASA Great Observatory open to proposals from the entire astronomical community. Please propose your brilliant observations !!!!

Backup Slides

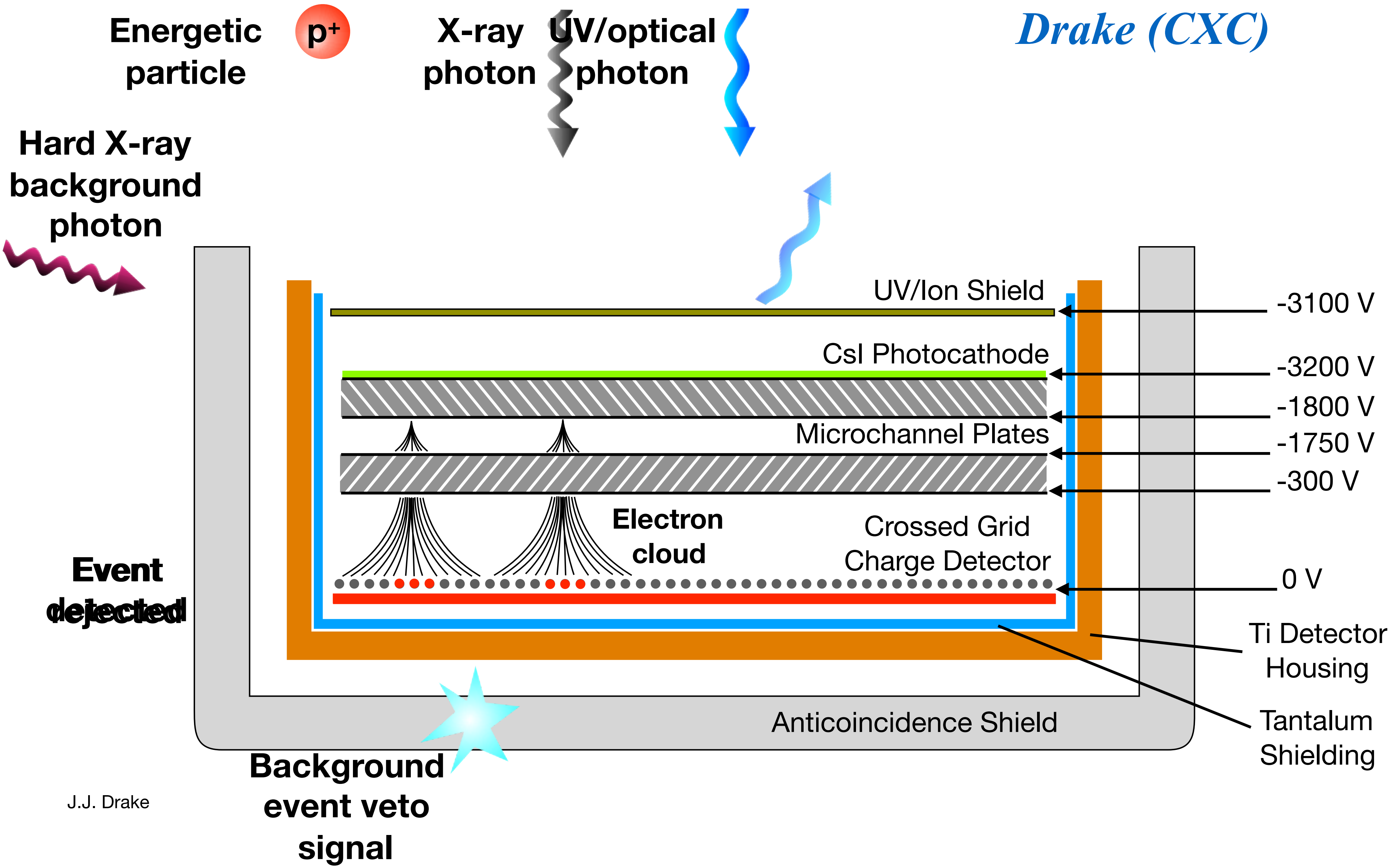
Energetic particle
p+
X-ray photon
UV/optical photon
Drake (CXC)
Hard X-ray background photon
UV/Ion Shield
CsI Photocathode
Microchannel Plates
Electron cloud
Crossed Grid Charge Detector
-3100 V
-3200 V
-1800 V
-1750 V
-300 V
0 V
Event
Ti Detector Housing
Tantalum Shielding
Anticoincidence Shield
Background event veto signal
J.J. Drake